PAPER

Periodic surface identification with phase or phaseless near-field data

To cite this article: Jinchang Zheng *et al* 2017 *Inverse Problems* **33** 115004

View the article online for updates and enhancements.

Periodic surface identification with phase or phaseless near-field data

Jinchang Zheng[1], Jin Cheng[1], Peijun Li[2] and Shuai Lu[1,3]

[1] School of Mathematical Sciences, Fudan University, Shanghai 200433,
People's Republic of China
[2] Department of Mathematics, Purdue University, West Lafayette, IN 47907,
United States of America

E-mail: 13110840006@fudan.edu.cn, jcheng@fudan.edu.cn,
lipeijun@math.purdue.edu and slu@fudan.edu.cn

Abstract

We investigate the inverse diffraction grating problem which is to reconstruct the periodic surface from the diffracted field. The surface is assumed to be a sufficiently smooth and small perturbation of the flat surface. A novel computational method is developed to solve the inverse problem with super-resolution by using phase or phaseless near-field data. The method utilizes Rayleigh's coefficients of the near field data and updates iteratively the approximated surface function by solving a truncated linearized system. Monotonicity of the error estimate is proved under the small perturbation assumption of the surface. Numerical examples are shown to verify the theoretical findings and illustrate the effectiveness of the proposed method.

Keywords: inverse diffraction grating problem, the Helmholtz equation, near-field imaging

(Some figures may appear in colour only in the online journal)

1. Introduction

Scattering theory in periodic structures has many significant applications in micro-optics, which includes the design and fabrication of optical elements such as corrective lenses, electronic displays, microsensors, optical storage systems, optical communication components, and integrated opto-electronic semiconductor devices [4, 5, 7, 22, 24, 39–41]. Surface identification of periodic structures is one of the fundamental problems in diffractive optics and is known as the inverse diffraction grating problem. The mathematical questions on uniqueness and stability for the inverse problem have been studied by many researchers [1, 3, 8, 15–17, 28, 33, 35]. Various numerical methods have also been developed for the reconstruction of

[3] Author to whom any correspondence should be addressed.

periodic surfaces [2, 14, 18, 23, 27, 29, 30, 36, 38, 42, 43, 46]. These works were intended to address the classical inverse scattering problems and the resolution of reconstructions was limited by Rayleigh's criterion, approximately half of the incident wavelength.

The resolution limit, referring to how fine the details can be captured, is an essential aspect to be considered in imaging and inverse scattering. It imposes an upper bound for the smallest resolvable features that can be seen for conventional far-field optics. To circumvent this difficulty, the near-field optics provides an effective approach to improve the resolution. By bringing the scanning device close to the samples, the non-radiative components, which does not propagate to the far-field detector, are captured, and sub-wavelength features can be obtained by exploiting these evanescent waves. This super-resolving capability makes near-field optics particularly attractive [19].

Recently, a novel approach has been developed to solve the inverse surface scattering problems in various near-field imaging modalities [6, 9–11, 13, 21, 31]. Under the small perturbation assumption of the surfaces, the method combined the transformed field expansion and Fourier analysis to find analytical solutions for the direct problems. Based on the analytical solutions and spectral cut-off regularization, explicit reconstruction formulas were derived for the linearized inverse problems. Subwavelength resolution was achieved stably by using the near-field data. The method requires both the phase and amplitude information for the data.

In practice, it might be cumbersome, if not impossible, to get the phase information when measuring the scattering data. It raises an interesting and challenging question on how to solve the inverse scattering problems by using the phaseless data only. An attempt was made to solve the inverse diffraction grating problem with phaseless data [12]. It has recently received much attention to solve various inverse scattering problems by using the data without phase information [20, 34, 37, 44, 45].

In this paper, we propose a novel computational method to solve the inverse diffraction grating problem. The goal is to achieve stably the super-resolution with phase or phaseless near-field data. According to Rayleigh's expansion, the total field is a combination of propagating and evanescent wave components with different spatial frequencies. In the Rayleigh series, each term is induced by different details or spatial frequencies of the scattering surface. More precisely, the *k*th Fourier coefficient of the scattering surface is related to the *k*th Rayleigh coefficient of the total field. Motivated by this observation, we use the Rayleigh expansion to extract the surface information from the scattering data. We emphasize that the conversion of the Rayleigh series is independent of each frequency, and higher order terms in Rayleigh series are more sensitive to the noise than lower order terms. Given a fixed measurement height, we may determine the highest cut-off index in the Rayleigh series such that the finest details of the surface are fully recovered even when the data contains a certain amount of noise.

In near-field optics, many applications are related to the so-called subsurface imaging, where it is reasonable to assume small amplitude of the surfaces. Our algorithm seeks to update the surface with small amplitudes iteratively. Based on Green's identity and eigenfunctions of the Helmholtz equation, an efficient direct solver is presented to determine the Rayleigh series with respect to the surface function. Our method also works for the phaseless data. Usually, it is impossible to recover the surface by using phaseless data with a single measure since the uniqueness is not guaranteed. But the situation is different for the near-field optics due to the assumption that the surface is a small perturbation of a flat plane. Based on this feature, we propose an energy assumption on the Rayleigh series, where a unique solution of the Rayleigh expansion can be obtained by a single phaseless measurement. In addition, we show the monotonicity of the error estimate between the exact surface and the reconstructed surface. Numerical examples are presented for both phase and phaseless data to illustrate the effectiveness of the proposed method.

The rest of the paper is organized as follows. In section 2, we introduce the model for the diffraction grating problem. Section 3 is devoted to the inverse problem and the reconstruction
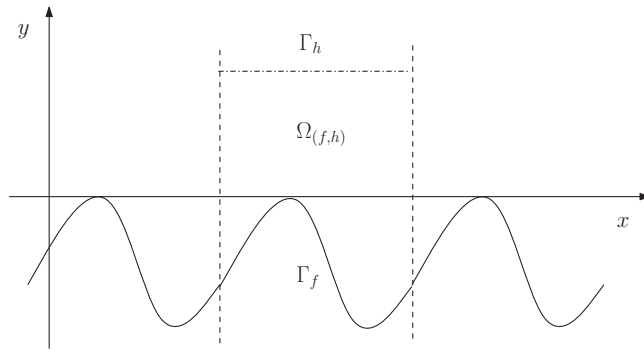
Figure 1. A schematic of the problem geometry.

algorithm. The error estimate is presented in section 4. Numerical experiments are shown in section 5. The paper is concluded with some general remarks in section 6.

2. Forward problem

In this section, we introduce the forward model for the underlying diffraction problem and present a formula to compute the coefficients in Rayleigh's expansion.

2.1. Problem formulation

Let us first introduce the problem geometry which is shown in figure 1. We assume that the structure is invariant in the z direction and is periodic in the x direction with period Λ. Denote the scattering surface in one period by

$$\Gamma_f = \{(x,y) \in \mathbb{R}^2 : y = f(x), \, x \in [0, \Lambda]\},$$

where $f \in C_{\mathrm{p}}^2([0,\Lambda])$ is a periodic function with period Λ. Here $C_{\mathrm{p}}^2([0,\Lambda])$ is the space of periodic functions with period Λ which are defined on the real axis and have second order continuous derivatives. Without loss of generality, we may assume that

$$\max_{x \in [0,\Lambda]} f(x) \leqslant 0.$$

To specify a boundary condition on Γ_f, we assume that the surface is a perfect electric conductor, i.e. a homogeneous Dirichlet boundary condition is imposed for the total wave field:

$$u = 0 \quad \text{on } \Gamma_f. \tag{2.1}$$

Denote the open space above the scattering surface by

$$\Omega_f = \{(x,y) \in \mathbb{R}^2 : y > f(x), \, x \in [0, \Lambda]\}.$$

The open space is filled with a homogeneous medium which may be characterized by a positive constant wavenumber κ. The wavelength is defined by $\lambda = 2\pi/\kappa$. Let

$$\Gamma_h = \{(x,y) \in \mathbb{R}^2 : y = h, \, x \in [0, \Lambda]\},$$

where $h > 0$ is a positive constant. In particular, Γ_h is the line of measurement, where $h > 0$ is called the measurement height. Denote the bounded domain

$$\Omega_{[f,h]} = \{(x,y) \in \mathbb{R}^2 : f(x) < y < h, \, x \in [0, \Lambda]\}.$$

As an application in near-field optics, the scattering surface is assumed to be small compared with the wavelength, i.e.

$$\max_{x \in [0, \Lambda]} |f(x)|/\lambda = \mathcal{O}(\epsilon),$$

where $0 < \epsilon \ll 1$ is called the surface deformation parameter.

Let a plane wave $u^{\text{inc}}(x, y) = e^{i(\alpha x - \beta y)}$ be incident on Γ_f from above, where $\alpha = \kappa \sin \theta$, $\beta = \kappa \cos \theta$ and $\theta \in (-\pi/2, \pi/2)$ is the incident angle. Since our method requires a single illumination, we take the most convenient experimental configuration and let the incidence to be normal, i.e. $\theta = 0$. The incident wave reduces to $u^{\text{inc}}(x, y) = e^{-i\kappa y}$.

In the transverse electric polarization, the total wave field u satisfies the two-dimensional Helmholtz equation:

$$\Delta u + \kappa^2 u = 0 \quad \text{in } \Omega_f. \tag{2.2}$$

The following radiation condition is imposed: the total field consists of the incident field and bounded outgoing waves in Ω_f. It follows from the outgoing radiation condition that the total field admits the Rayleigh expansion:

$$u(x, y) = e^{-i\kappa y} + \sum_{n \in \mathbb{Z}} A_n e^{i(\alpha_n x + \beta_n y)}, \quad y > 0, \tag{2.3}$$

where

$$A_n \in \mathbb{C}, \quad \alpha_n = n \left(\frac{2\pi}{\Lambda} \right), \quad \beta_n = \begin{cases} (\kappa^2 - \alpha_n^2)^{1/2}, & |\alpha_n| < \kappa, \\ i(\alpha_n^2 - \kappa^2)^{1/2}, & |\alpha_n| > \kappa. \end{cases} \tag{2.4}$$

Here, we assume that $|\alpha_n| \neq \kappa, n \in \mathbb{Z}$ to exclude possible resonance. Physically, the Rayleigh expansion (2.3) shows that the wave field is a superposition of plane waves which include finitely many propagating wave modes and infinitely many evanescent wave modes. The evanescent waves are also called the surface waves which propagate along the x-axis and decay exponentially along the y-axis.

Taking the partial derivative of (2.3) with respect to y and evaluating at $y = h$, we may obtain the transparent boundary condition:

$$\partial_y u = Tu - 2i\kappa e^{-i\kappa h} \quad \text{on } \Gamma_h,$$

where the Dirichlet-to-Neumann (DtN) operator T is defined by

$$(Tu)(x, h) = \sum_{n \in \mathbb{Z}} i\beta_n u^{(n)} e^{i\alpha_n x}, \quad u(x, h) = \sum_{n \in \mathbb{Z}} u^{(n)} e^{i\alpha_n x}.$$

In summary, the diffractive grating model can be formulated into the following boundary value problem:

$$\begin{cases} \Delta u + \kappa^2 u = 0 & \text{in } \Omega_{[f,h]} \\ u = 0 & \text{on } \Gamma_f \\ \partial_y u = Tu - 2i\kappa e^{-i\kappa h} & \text{on } \Gamma_h. \end{cases} \tag{2.5}$$

It is known in [32] that the boundary value problem (2.5) admits a unique periodic solution $u \in C_p^2(\Omega_{[f,h]}) \cap C_p^1(\bar{\Omega}_{[f,h]})$ if $f \in C_p^2([0, \Lambda])$. Clearly, we have the following regularity for the solution: $u \in H_p^2(\Omega_{[f,h]}), u \in H^{3/2}(\Gamma_f), \partial_\nu u \in H^{1/2}(\Gamma_f)$, where ν is the unit outward normal on Γ_f.

2.2. Rayleigh's coefficients

Recall Green's second identity for any two smooth functions u and v in a bounded Lipschitz domain Ω:

$$\int_{\Omega}(\Delta u\, v - \Delta v\, u)\mathrm{d}x\mathrm{d}y = \int_{\partial\Omega}(\partial_{\nu}u\, v - \partial_{\nu}v\, u)\mathrm{d}\gamma, \tag{2.6}$$

where ν is the unit outward normal on $\partial\Omega$. Consider the following two test functions:

$$G_n^+(x,y) = \mathrm{e}^{-\mathrm{i}(\alpha_n x - \beta_n y)}, \quad G_n^-(x,y) = \mathrm{e}^{-\mathrm{i}(\alpha_n x + \beta_n y)},$$

where α_n, β_n are defined in (2.4). It can be verified that the above two test functions satisfy the Helmholtz equation (2.2). Substituting $G_n^{\pm}$ and the solution u of the boundary value problem (2.5) into (2.6) over the domain $\Omega_{[f,h]}$ yields

$$\int_{\partial\Omega_{[f,h]}}(\partial_{\nu}u G_n^{\pm} - \partial_{\nu}G_n^{\pm}u)\mathrm{d}\gamma = 0.$$

As seen in figure 2, the boundary $\partial\Omega_{[f,h]} = \Gamma_f \cup \Gamma_h \cup \gamma_1 \cup \gamma_2$. Since both $G_n^{\pm}(x,y)$ and $u(x,y)$ are periodic in x, it is easy to show that

$$\left(\int_{\gamma_1} + \int_{\gamma_2}\right)(\partial_{\nu}u G_n^{\pm} - \partial_{\nu}G_n^{\pm}u)\mathrm{d}\gamma = 0.$$

Following from Rayleigh's expansion (2.3), we have for all $n \in \mathbb{N}$ that

$$\int_{\Gamma_h}(\partial_y u G_n^+ - \partial_y G_n^+ u)\mathrm{d}x = -2\mathrm{i}\kappa\Lambda\delta_{0n}, \tag{2.7}$$

$$\int_{\Gamma_h}(\partial_y u G_n^- - \partial_y G_n^- u)\mathrm{d}x = 2\mathrm{i}\beta_n\Lambda A_n, \tag{2.8}$$

where δ_{0n} is the Kronecker delta. Noting that $\partial_{\nu}u \in H^{1/2}(\Gamma_f)$ is periodic in x with period Λ, we can expand $(1+(f')^2)^{1/2}\partial_{\nu}u$ into the Fourier series:

$$(1+(f'(x))^2)^{1/2}\partial_{\nu}u(x,f(x)) = \sum_{m\in\mathbb{Z}}B_m\mathrm{e}^{\mathrm{i}\alpha_m x}, \quad B_m \in \mathbb{C}. \tag{2.9}$$

Substituting (2.9) into the integral along Γ_f, we get for all $n \in \mathbb{N}$ that

$$\int_{\Gamma_f}\partial_{\nu}u G_n^+\mathrm{d}\gamma = \sum_{m\in\mathbb{Z}}B_m\int_0^{\Lambda}\mathrm{e}^{\mathrm{i}(\alpha_{m-n}x+\beta_n f(x))}\mathrm{d}x, \tag{2.10}$$

$$\int_{\Gamma_f}\partial_{\nu}u G_n^-\mathrm{d}\gamma = \sum_{m\in\mathbb{Z}}B_m\int_0^{\Lambda}\mathrm{e}^{\mathrm{i}(\alpha_{m-n}x-\beta_n f(x))}\mathrm{d}x. \tag{2.11}$$

Combining (2.7), (2.8) and (2.10), (2.11), and the boundary condition (2.1), we obtain a linear system of equations for A_n and B_m:

$$\sum_{m\in\mathbb{Z}}B_m\int_0^{\Lambda}\mathrm{e}^{\mathrm{i}(\alpha_{m-n}x+\beta_n f(x))}\mathrm{d}x = 2\mathrm{i}\kappa\Lambda\delta_{0n}, \tag{2.12}$$

$$\sum_{m\in\mathbb{Z}}B_m\int_0^{\Lambda}\mathrm{e}^{\mathrm{i}(\alpha_{m-n}x-\beta_n f(x))}\mathrm{d}x = -2\mathrm{i}\beta_n\Lambda A_n. \tag{2.13}$$
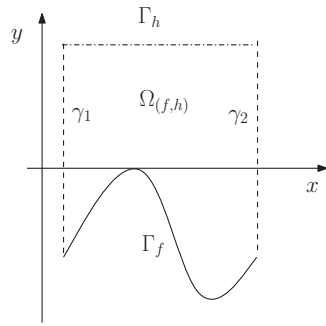
Figure 2. Schematic of the integral contour.

As can be observed in (2.9), the surface function $f(x)$ is implicitly represented in a form of the Fourier coefficients B_m. Our goal is to retrieve the surface information from the Fourier coefficients. The algorithm proposed in the next section is to linearize the above system (2.12) and (2.13) and update iteratively the approximated surface function $f(x)$.

3. Inverse problem

In this section, we discuss how to compute Rayleigh's coefficients A_n from either the phase or phaseless data, and then present an iterative reconstruction algorithm to solve the inverse problem.

3.1. Phase data

First we consider how to retrieve the Rayleigh coefficients from the phase data. Evaluating (2.3) at $y = h$, we have

$$\sum_{n\in\mathbb{Z}} A_n e^{i(\alpha_n x + \beta_n h)} = u(x,h) - e^{-i\kappa h}.$$

Using the orthogonality of the functions $e^{i\alpha_n x}$ on $[0, \Lambda]$, we may compute the coefficients A_n by

$$A_n = \frac{e^{-i\beta_n h}}{\Lambda} \int_0^\Lambda u(x,h)e^{-i\alpha_n x}\mathrm{d}x - e^{-i(\kappa+\beta_n)h}\delta_{0n}. \tag{3.1}$$

It follows from the definition of β_n in (2.4) and the conversion formula (3.1) that the measurement noise will be amplified exponentially for $|\alpha_n| > \kappa$. Therefore it is exponentially unstable to recover high frequency coefficients of A_n. Taking account of the stability, we take the measurement height h and the highest frequency mode n to satisfy $|e^{-i\beta_n h}| = \mathcal{O}(1)$.

3.2. Phaseless data

To retrieve the unique Rayleigh expansion coefficients from phaseless data, we impose the following extra energy conditions:

$$|A_0| = 1 \quad \text{and} \quad |A_m| = |A_{-m}|. \tag{3.2}$$

The real and imaginary parts of the Rayleigh coefficient A_0 can be solved from the following quadratic equation if we seek the solution around -1 for $\mathrm{Re}A_0$ such that

$$(\text{Re}A_0)^2 + (\text{Im}A_0)^2 = 1, \tag{3.3}$$

$$\frac{1}{2\Lambda} \int_0^\Lambda |u(x,h)|^2 \mathrm{d}x - 1 = \cos(2\kappa h)\text{Re}A_0 - \sin(2\kappa h)\text{Im}A_0 \tag{3.4}$$

and A_m, $m \neq 0$ via the pseudo-inverse method

$$\text{Re}A_m = \cos(\Phi_m)\text{Re}A_{-m} + \sin(\Phi_m)\text{Im}A_{-m}, \tag{3.5}$$

$$\text{Im}A_m = -\sin(\Phi_m)\text{Re}A_{-m} + \cos(\Phi_m)\text{Im}A_{-m} \tag{3.6}$$

where coefficients A_{-m} and A_m satisfy

$$\frac{1}{\Lambda} \int_0^\Lambda |u(x,h)|^2 \mathrm{e}^{\mathrm{i}\alpha_m x} \mathrm{d}x = \left(\mathrm{e}^{\mathrm{i}(\kappa + \beta_m)h} + \bar{A}_0 \mathrm{e}^{\mathrm{i}(-\kappa + \beta_m)h} \right) A_{-m} + \left(\mathrm{e}^{-\mathrm{i}(\kappa + \bar{\beta}_m)h} + A_0 \mathrm{e}^{\mathrm{i}(\kappa - \bar{\beta}_m)h} \right) \bar{A}_m \tag{3.7}$$

and Φ_m are the angles and satisfy

$$\tan\left(\frac{\Phi_m}{2}\right) = \text{Im}\left(\int_0^\Lambda |u(x,h)|^2 \mathrm{e}^{\mathrm{i}\alpha_m x} \mathrm{d}x \right) \Big/ \text{Re}\left(\int_0^\Lambda |u(x,h)|^2 \mathrm{e}^{\mathrm{i}\alpha_m x} \mathrm{d}x \right).$$

In appendix A.1, we provide more details concerning the derivation of (3.3)–(3.7).

3.3. Reconstruction method

We present an iterative method to reconstruct the scattering surface. The main idea is to linearize the system (2.12) and (2.13) and update the approximated surface function iteratively.

Let $f_0 = 0$ be the initial guess. Denote by f_ℓ the current approximated surface. We wish to determine the next approximation $f_{\ell+1}$, or equivalently, to determine the perturbation

$$f_{\ell+1}(x) - f_\ell(x) = \epsilon g(x), \tag{3.8}$$

where $g(x) = \mathcal{O}(\lambda)$.

Since the deformation parameter ϵ is small, we consider power series expansions:

$$B_m = \sum_{j=0}^\infty B_m^{(j)} \epsilon^j \tag{3.9}$$

and

$$\mathrm{e}^{\pm\mathrm{i}\beta_n f_{\ell+1}} = \mathrm{e}^{\pm\mathrm{i}\beta_n (f_\ell + \epsilon g)} = \mathrm{e}^{\pm\mathrm{i}\beta_n f_\ell} \mathrm{e}^{\pm\mathrm{i}\beta_n \epsilon g} = \mathrm{e}^{\pm\mathrm{i}\beta_n f_\ell(x)} \sum_{j=0}^\infty (\pm\mathrm{i}\beta_n g)^j \epsilon^j, \tag{3.10}$$

where B_m are the Fourier coefficients of $(1 + (f'(x))^2)^{1/2} \partial_\nu u(x, f(x))$ and $B_m^{(j)}$ is the jth expansion coefficient of B_m with respect to ϵ. Plugging (3.9) and (3.10) into (2.12) and (2.13) and dropping high order $\mathcal{O}(\epsilon^2)$ terms, we obtain a linearized system for (2.12) and (2.13):

$$\sum_{m\in\mathbb{Z}} \int_0^\Lambda \mathrm{e}^{\mathrm{i}(\alpha_{m-n}x + \beta_n f_\ell(x))} \left(B_m^{(0)} + \epsilon B_m^{(1)} + \mathrm{i}\beta_n B_m^{(0)} \epsilon g(x) \right) \mathrm{d}x = 2\mathrm{i}\kappa\Lambda\delta_{0n}, \tag{3.11}$$

$$\sum_{m\in\mathbb{Z}} \int_0^\Lambda \mathrm{e}^{\mathrm{i}(\alpha_{m-n}x - \beta_n f_\ell(x))} \left(B_m^{(0)} + \epsilon B_m^{(1)} - \mathrm{i}\beta_n B_m^{(0)} \epsilon g(x) \right) \mathrm{d}x = -2\mathrm{i}\beta_n\Lambda A_n \tag{3.12}$$

where the Rayleigh coefficient A_n can be obtained from the phase data $u(x, h)$ through (3.1) or the phaseless data $|u(x, h)|$ by (3.3)–(3.7). Coefficients $B_m^{(0)}$ is updated by fitting (2.12) with the interface $f_\ell(x)$.

Since the exact surface $f(x)$ is periodic, we assume that both $f_\ell(x)$ and $\epsilon g(x)$ are periodic too. More precisely, we can expand $\epsilon g(x)$ into the Fourier series:

$$\epsilon g(x) = \sum_{k \in \mathbb{Z}} C_k e^{i\alpha_k x}. \tag{3.13}$$

Our goal is to recover the Fourier coefficients C_k. Substituting the Fourier series (3.13) into (3.11) and (3.12) yields

$$\sum_{m \in \mathbb{Z}} \int_0^\Lambda e^{i(\alpha_{m-n}x + \beta_n f_\ell(x))} \left(B_m^{(0)} + \epsilon B_m^{(1)} + i\beta_n B_m^{(0)} \sum_{k \in \mathbb{Z}} C_k e^{i\alpha_k x} \right) dx = 2i\kappa\Lambda\delta_{0n}, \tag{3.14}$$

$$\sum_{m \in \mathbb{Z}} \int_0^\Lambda e^{i(\alpha_{m-n}x - \beta_n f_\ell(x))} \left(B_m^{(0)} + \epsilon B_m^{(1)} - i\beta_n B_m^{(0)} \sum_{k \in \mathbb{Z}} C_k e^{i\alpha_k x} \right) dx = -2i\beta_n\Lambda A_n, \tag{3.15}$$

where $\epsilon B_m^{(1)}$ and C_k are unknown variables. Solving the linear system (3.14) and (3.15), we can finally obtain the Fourier coefficients C_k of the increment $\epsilon g(x)$ which is then added to $f_\ell(x)$ to iteratively generated the approximate surface function $f_{\ell+1}(x)$.

We summarize the algorithm as below.

Algorithm 1. Surface identification algorithm.

Input: Measurement of phase data $u(x, h)$ or phaseless data $|u(x, h)|$, truncated number N for the Rayleigh expansion, max iterative number L.

Output: Updated surface function $f_{\ell,N}(x)$.

1: Set $f_0(x) = 0$;

2: Convert the measurement into the Rayleigh coefficients A_n by (3.1) or (3.3)–(3.7),
     $n = 0, \pm 1, \pm 2, \ldots, \pm N$;

3: **For** $\ell = 1, 2, \ldots, L$

4:      Solve the direct problem (2.12) with $f_{\ell,N}(x)$ as

$$\sum_{m=-N}^N \left(\int_0^\Lambda e^{i(\alpha_{m-n}x + \beta_n f_{\ell,N}(x))} dx \right) B_m^{(0)} = 2i\kappa\Lambda\delta_{0n}, \quad n = 0, \pm 1, \ldots, \pm N \tag{3.16}$$

to obtain the coefficients $B_m^{(0)}, m = 0, \pm 1, \ldots, \pm N$;

5:      Find the surface increment $\epsilon g_{\ell,N}(x) = \sum_{k=-N}^N C_{\ell+1,k} e^{i\alpha_k x}$ and the auxiliary variables $B_k^{(1)}$,
     $k = 0, \pm 1, \ldots, \pm N$ by solving the linearized system (3.14) and (3.15):

$$\sum_{k=-N}^N \left(\int_0^\Lambda e^{i(\alpha_{k-n}x + \beta_n f_{\ell,N}(x))} dx \right) B_k^{(1)} + i\beta_n \sum_{k=-N}^N \left(\sum_{m=-N}^N \int_0^\Lambda e^{i(\alpha_{m+k-n}x + \beta_n f_{\ell,N}(x))} B_m^{(0)} dx \right) C_{\ell+1,k}$$

$$= 2i\kappa\Lambda\delta_{0n} - \sum_{m=-N}^N \left(\int_0^\Lambda e^{i(\alpha_{m-n}x + \beta_n f_{\ell,N}(x))} dx \right) B_m^{(0)}, \tag{3.17}$$

$$\sum_{k=-N}^N \left(\int_0^\Lambda e^{i(\alpha_{k-n}x - \beta_n f_{\ell,N}(x))} dx \right) B_k^{(1)} - i\beta_n \sum_{k=-N}^N \left(\sum_{m=-N}^N \int_0^\Lambda e^{i(\alpha_{m+k-n}x - \beta_n f_{\ell,N}(x))} B_m^{(0)} dx \right) C_{\ell+1,k}$$

$$= -2i\beta_n\Lambda A_n - \sum_{m=-N}^N \left(\int_0^\Lambda e^{i(\alpha_{m-n}x - \beta_n f_{\ell,N}(x))} dx \right) B_m^{(0)}. \tag{3.18}$$

6:      Update the scattering surface $f_{\ell+1,N}(x) = f_{\ell,N}(x) + \epsilon g_{\ell,N}(x)$;

7: **End**

---

4. Error estimate

In this section, we estimate the error between the updated surface function $f_{\ell+1,N}(x)$ and the exact one f. The notation $f \lesssim g$ for two functions stands for $f \leqslant Cg$ where $C > 0$ is a generic constant.

4.1. Auxiliary lemmas

Let the initial guess $f_0(x) = 0$. Our algorithm produces $f_{\ell+1,N}(x)$ at $(\ell+1)$th step via the formula

$$f_{\ell+1,N}(x) = f_{\ell,N}(x) + \sum_{n=-N}^{N} C_{\ell+1,n} e^{i\alpha_n x}, \tag{4.1}$$

where $C_{\ell+1,n}$ is updated from $(\ell+1)$th iteration of Algorithm 1. On the other hand, the exact interface can also be expressed in term of $f_{\ell,N}$

$$f(x) = f_{\ell,N}(x) + \sum_{n=-\infty}^{\infty} C_n e^{i\alpha_n x}. \tag{4.2}$$

We truncate $2N+1$ terms of the Fourier series of the exact surface $f(x)$ and denote it by

$$f_N(x) = f_{\ell,N}(x) + \sum_{n=-N}^{N} C_n e^{i\alpha_n x}.$$

Subtracting (4.2) from (4.1), we may easily verify that

$$\|f_{\ell+1,N} - f\|_{H^2(0,\Lambda)} \lesssim \|f_{\ell+1,N} - f_N\|_{H^2(0,\Lambda)} + \|f - f_N\|_{H^2(0,\Lambda)}$$

$$\lesssim \left(\sum_{n=-N}^{N} n^4 |C_{\ell+1,n} - C_n|^2 \right)^{1/2} + \|f - f_N\|_{H^2(0,\Lambda)}. \tag{4.3}$$

The truncated error $\|f - f_N\|_{H^2(0,\Lambda)}$ is fixed for our algorithm, so we mainly focus on the error bound for the computed part $|C_{\ell+1,n} - C_n|$ with $|n| \leqslant N$, i.e. the error bound of $\|f_{\ell+1,N} - f_N\|_{H^2(0,\Lambda)}$.

First, we introduce the following lemma, which allows a well-defined expansion formula (3.9). The proof is given in appendix A.2.

Lemma 4.1. *Assume that the surface functions $f_j \in C_p^2([0,\Lambda])$ satisfy $\|f_j\|_{H^2(0,\Lambda)} \lesssim \epsilon$, $f_j \leqslant 0$ and*

$$\|f_1 - f_2\|_{H^2(0,\Lambda)} \lesssim \tau. \tag{4.4}$$

Let

$$\Omega_j = \left\{ (x,y) \in \mathbb{R}^2 | 0 \leqslant x \leqslant \Lambda, f_j(x) \leqslant y \leqslant 1 \right\}.$$

Then, the solutions u_j of (2.5) in Ω_j satisfy

$$\left\| (1 + (f_1')^2)^{1/2} \partial_{\nu_1} u_1 - (1 + (f_2')^2)^{1/2} \partial_{\nu_2} u_2 \right\|_{H^{1/2}(0,\Lambda)} \lesssim \tau,$$

where ν_j are the unit outward normal vectors on Γ_{f_j}.

The above lemma suggests that a small perturbation of the scattering surface gives a small change of the normal derivative on Γ_f. This lemma allows to quantify the difference between the exact surface f and the updated surface $f_{\ell+1,N}$. Meanwhile, the following lemma is needed to quantify the error of the mth Fourier mode $B_{m,N}$ of $(1 + (f'_{\ell,N})^2)^{1/2}\partial_\nu u_\ell(x, f_{\ell,N})$ and $B_m^{(0)}$ of the power series (3.16). The proof is presented in appendix A.2.

Lemma 4.2. *Let N be the cut-off parameter in (3.16). Suppose $f_{\ell,N}(x) \in C_p^2([0, \Lambda])$ satisfying*

$$\|f_{\ell,N}\|_{H^2(0,\Lambda)} < \frac{\epsilon}{\max\{\sqrt{\Lambda}, 1/\sqrt{\Lambda}\}}.$$

Let u be the solution of (2.5) and $\partial_\nu u$ be the normal derivative of u at $\Gamma_{f_{\ell,N}}$ with

$$(1 + (f'_{\ell,N})^2)^{1/2}\partial_\nu u = \sum_{m \in \mathbb{Z}} B_{m,N} e^{i\alpha_n x}.$$

If the deformation parameter ϵ is sufficiently small such that

$$\epsilon \max_{n \in [-N,N]} |\beta_n| < \min\{\Lambda, 1\}/6\pi^2, \quad n = 0, \pm 1, \ldots, \pm N, \tag{4.5}$$

then the difference between $B_{m,N}$ and $B_m^{(0)}$ satisfies

$$|B_{m,N} - B_m^{(0)}| \lesssim \epsilon^2 N^{-1/2} \max_{n \in [-N,N]} |\beta_n|.$$

4.2. Monotonicity of the error estimate

In the error analysis, one of the key steps is to estimate

$$|C_{\ell+1,n} - C_n|, \quad n = 0, \pm 1 \ldots, \pm N.$$

Since the goal of this work is to address the super-resolution, we may assume that $\kappa < 2\pi/\Lambda$, which gives $|\beta_n| \sim n$. Now we present the monotonicity of the error estimate for $\ell + 1$ step in algorithm 1.

Theorem 4.3. *Let $f(x)$ and $f_{\ell,N}(x)$ be the exact surface and the approximated surface at ℓ th step, respectively. If $f(x)$ and $f_{\ell,N}(x)$ satisfy*

$$\|f\|_{H^2(0,\Lambda)} \lesssim \epsilon, \quad \|f_{\ell,N}\|_{H^2(0,\Lambda)} \lesssim \epsilon, \quad \|f_{\ell,N} - f\|_{H^2(0,\Lambda)} \lesssim \tau,$$

and

$$\epsilon N^2 = \mathcal{O}(1), \quad \tau \lesssim \epsilon, \tag{4.6}$$

then

$$|C_{\ell+1,n} - C_n| \lesssim (\epsilon^2 + \tau^2 + \epsilon\|f - f_N\|_{H^2(0,\Lambda)})(1 + |n|)^{-1/2}$$

and

$$\|f_{\ell+1,N} - f\|_{H^2(0,\Lambda)} \lesssim (\epsilon^2 + \tau^2)N^2 + \|f - f_N\|_{H^2(0,\Lambda)}.$$

Proof. For $n = 0, \pm 1, \ldots, \pm N$, we reformulate the forward problem (2.12) and (2.13) as follows

$$\sum_{k=-N}^{N} \left(\int_0^\Lambda e^{i(\beta_n f_{\ell,N} + \alpha_{k-n}x)} dx \right) (B_k - B_k^{(0)}) + i\beta_n \sum_{m=-N}^{N} \int_0^\Lambda B_m^{(0)} (f_N - f_{\ell,N}) e^{i(\beta_n f_{\ell,N} + \alpha_{m-n}x)} dx$$

$$= 2i\kappa\Lambda\delta_{0n} - \sum_{m=-N}^{N} \left(\int_0^\Lambda e^{i(\beta_n f_{\ell,N} + \alpha_{m-n}x)} dx \right) B_m^{(0)} + b_n^{(1)}$$

and

$$\sum_{k=-N}^{N} \left(\int_0^\Lambda e^{i(-\beta_n f_{\ell,N} + \alpha_{k-n}x)} dx \right) (B_k - B_k^{(0)}) - i\beta_n \sum_{m=-N}^{N} \int_0^\Lambda B_m^{(0)} (f_N - f_{\ell,N}) e^{i(-\beta_n f_{\ell,N} + \alpha_{m-n}x)} dx$$

$$= -2i\beta_n\Lambda A_n - \sum_{m=-N}^{N} \left(\int_0^\Lambda e^{i(-\beta_n f_{\ell,N} + \alpha_{m-n}x)} dx \right) B_m^{(0)} + b_n^{(2)},$$

where f_N is the truncated Fourier series of f and $b_n^{(i)}$, $i = 1, 2$ is defined as

$$b_n^{(i)} = - \sum_{m=-\infty}^{\infty} \left(\int_0^\Lambda e^{i\left((-1)^{i-1}\beta_n f_{\ell,N} + \alpha_{m-n}x\right)} \left(e^{(-1)^{i-1}i\beta_n(f-f_{\ell,N})} - 1 - (-1)^{i-1}i\beta_n \left(f - f_{\ell,N} \right) \right) dx \right) B_m$$

$$- \sum_{|m|>N} \left(\int_0^\Lambda e^{i\left((-1)^{i-1}\beta_n f_{\ell,N} + \alpha_{m-n}x\right)} \left(1 + (-1)^{i-1}i\beta_n \left(f - f_{\ell,N} \right) \right) dx \right) B_m$$

$$+ (-1)^{i-1}i\beta_n \sum_{m=-N}^{N} \left(\int_0^\Lambda e^{i\left((-1)^{i-1}\beta_n f_{\ell,N} + \alpha_{m-n}x\right)} \left(f - f_{\ell,N} \right) dx \right) (B_m^{(0)} - B_m)$$

$$- (-1)^{i-1}i\beta_n \sum_{m=-N}^{N} \int_0^\Lambda B_m^{(0)} (f - f_N) e^{i\left((-1)^{i-1}\beta_n f_{\ell,N} + \alpha_{m-n}x\right)} dx. \tag{4.7}$$

The estimates of $b_n^{(i)}$ are given in lemma B.3.

Subtracting (3.17) and (3.18) from above equalities and noticing that

$$f_N - f_{\ell,N} = \sum_{k=-N}^{N} C_k e^{i\alpha_k x},$$

we get a linear system for $C_k - C_{\ell+1,k}$, $k = 0, \pm 1, \ldots, \pm N$:

$$\sum_{k=-N}^{N} a_{n,k}^{(1)} (B_k - B_k^{(0)} - B_{\ell+1,k}^{(1)}) + \sum_{k=-N}^{N} a_{n,k}^{(3)} (C_k - C_{\ell+1,k}) = b_n^{(1)}, \tag{4.8}$$

$$\sum_{k=-N}^{N} a_{n,k}^{(2)} (B_k - B_k^{(0)} - B_{\ell+1,k}^{(1)}) + \sum_{k=-N}^{N} a_{n,k}^{(4)} (C_k - C_{\ell+1,k}) = b_n^{(2)}, \tag{4.9}$$

where $a_n^{(j)}$, $j = 1, \ldots, 4$ are defined as

$$a_{n,k}^{(1)} = \int_0^\Lambda e^{i(\beta_n f_{\ell,N} + \alpha_{k-n} x)} dx,$$

$$a_{n,k}^{(2)} = \int_0^\Lambda e^{i(-\beta_n f_{\ell,N} + \alpha_{k-n} x)} dx,$$

$$a_{n,k}^{(3)} = i\beta_n \sum_{m=-N}^N \int_0^\Lambda e^{i(\beta_n f_{\ell,N} + \alpha_{m+k-n} x)} B_m^{(0)} dx,$$

$$a_{n,k}^{(4)} = -i\beta_n \sum_{m=-N}^N \int_0^\Lambda e^{i(-\beta_n f_{\ell,N} + \alpha_{m+k-n} x)} B_m^{(0)} dx.$$

The factor $i\beta_n$ in $a_{n,k}^{(3)}$ and $a_{n,k}^{(4)}$ can affect the sharpness of our method used in lemma 4.2. To circumvent this difficulty, we scale $C_k - C_{\ell+1,k}$ with $|k| + 1$ such that linear system (4.8) and (4.9) is transformed into

$$\sum_{k=-N}^N \hat{a}_{n,k}^{(1)}(B_k - B_k^{(0)} - B_{\ell+1,k}^{(1)}) + \sum_{k=-N,k\neq 0}^N \hat{a}_{n,k}^{(3)}(|k|+1)(C_k - C_{\ell+1,k}) = b_n^{(1)}, \tag{4.10}$$

$$\sum_{k=-N,k\neq 0}^N \hat{a}_{n,k}^{(2)}(B_k - B_k^{(0)} - B_{\ell+1,k}^{(1)}) + \sum_{k=-N,k\neq 0}^N \hat{a}_{n,k}^{(4)}(|k|+1)(C_k - C_{\ell+1,k}) = b_n^{(2)}, \tag{4.11}$$

with

$$\hat{a}_{n,k}^{(1)} = a_{n,k}^{(1)}, \quad \hat{a}_{n,k}^{(2)} = a_{n,k}^{(2)}, \quad \hat{a}_{n,k}^{(3)} = a_{n,k}^{(3)}/(|k|+1), \quad \hat{a}_{n,k}^{(4)} = a_{n,k}^{(4)}/(|k|+1).$$

Their estimates can be found in lemmas B.1 and B.2.

Let $x_k^{(1)} = (B_k - B_k^{(0)} - B_{\ell+1,k}^{(1)})$ and $x_k^{(2)} = (|k|+1)(C_k - C_{\ell+1,k})$. The linear system (4.10) and (4.11) can be written into the matrix form:

$$\begin{pmatrix} A^{(1)} & A^{(3)} \\ A^{(2)} & A^{(4)} \end{pmatrix} \begin{pmatrix} x^{(1)} \\ x^{(2)} \end{pmatrix} = \begin{pmatrix} b^{(1)} \\ b^{(2)} \end{pmatrix},$$

where $x^{(j)} = (x_{-N}^{(j)}, x_{-N+1}^{(j)}, \ldots, x_N^{(j)})^\top$, $y^{(j)} = (y_{-N}^{(j)}, y_{-N+1}^{(j)}, \ldots, y_N^{(j)})^\top$, and

$$A^{(j)} = \begin{pmatrix} \hat{a}_{-N,-N}^{(j)} & \hat{a}_{-N,-N+1}^{(j)} & \cdots & \hat{a}_{-N,N}^{(j)} \\ \hat{a}_{-N,-N}^{(j)} & \hat{a}_{-N,-N+1}^{(j)} & \cdots & \hat{a}_{-N,N}^{(j)} \\ \vdots & \vdots & \ddots & \vdots \\ \hat{a}_{N,-N}^{(j)} & \hat{a}_{N,-N+1}^{(j)} & \cdots & \hat{a}_{N,N}^{(j)} \end{pmatrix}.$$

Let $A^{(i)} = \text{diag}A^{(i)} + \delta A^{(i)}$, where $\text{diag}A^{(i)}$ is the diagonal matrix of $A^{(i)}$ and $\delta A^{(i)}$ is its off-diagonal matrix. Then, we decompose A into a block diagonal matrix with small perturbation as $A = \text{diag}A + \delta A$, where

$$\text{diag}A = \begin{pmatrix} \text{diag}A^{(1)} & \text{diag}A^{(3)} \\ \text{diag}A^{(2)} & \text{diag}A^{(4)} \end{pmatrix}, \quad \delta A = \begin{pmatrix} \delta A^{(1)} & \delta A^{(3)} \\ \delta A^{(2)} & \delta A^{(4)} \end{pmatrix}.$$

Define

$$T^{(1)} = (\text{diag}A^{(1)})^{-1} + (\text{diag}A^{(1)})^{-1}\text{diag}A^{(3)}T^{(4)}\text{diag}A^{(2)}(\text{diag}A^{(1)})^{-1},$$
$$T^{(2)} = -T^{(4)}\text{diag}A^{(2)}(\text{diag}A^{(1)})^{-1},$$
$$T^{(3)} = -(\text{diag}A^{(1)})^{-1}\text{diag}A^{(3)}T^{(4)},$$
$$T^{(4)} = \left(\text{diag}A^{(4)} - \text{diag}A^{(2)}(\text{diag}A^{(1)})^{-1}\text{diag}A^{(3)}\right)^{-1}.$$

Denote $t_{n,n}^{(1)}, t_{n,n}^{(2)}, t_{n,n}^{(3)}, t_{n,n}^{(4)}$ be their corresponding diagonal entries. A direct calculation yields

$$\text{diag}A^{-1} = \begin{pmatrix} T^{(1)} & T^{(3)} \\ T^{(2)} & T^{(4)} \end{pmatrix}.$$

The invertibility of $\text{diag}A$ is guaranteed by the lower bound in lemma B.2 when λ/Λ is not an integer.

Noting that the assumption (4.5) can be obtained by the assumption (4.6), we derive from lemma B.2 that there exists a positive constant C independent on ϵ, h and N such that

$$\frac{1}{|t_{n,n}^{(4)}|} = |\hat{a}_{n,n}^{(4)} - \hat{a}_{n,n}^{(2)}\hat{a}_{n,n}^{(3)}/\hat{a}_{n,n}^{(1)}| \geqslant \frac{|\beta_n|}{(|n|+1)}\left(\frac{4}{3}\kappa\Lambda^2 - C\epsilon|\beta_n|\right).$$

It follows from (4.6) that

$$\frac{1}{3}\kappa\Lambda^2 > C\epsilon|\beta_n|,$$

which gives that

$$|t_{n,n}^{(1)}|, \ |t_{n,n}^{(3)}| \lesssim 1, \quad |t_{n,n}^{(2)}|, \ |t_{n,n}^{(4)}| \lesssim \frac{(|n|+1)}{|\beta_n|} \lesssim 1. \tag{4.12}$$

It is easy to verify the following fundamental estimates:

$$\sum_{k=1}^{N}\frac{1}{k} \leqslant \int_1^N x^{-1}\mathrm{d}x + 1 \lesssim \ln N,$$

$$\sum_{k=-N,k\neq n}^{N}\frac{1}{(|k|+1)|n-k|^{1/2}} \lesssim \int_0^{|n|-1} + \int_{|n|+1}^{\infty}\frac{1}{(x+1)(|n|-x)^{1/2}} \lesssim 1,$$

$$\sum_{k=-N,k\neq n}^{N}\frac{|\beta_n|}{(|k|+1)(n-k)^2} \sim \sum_{k=0,k\neq n}^{N}\frac{|n|}{(k+1)(|n|-k)^2}$$

$$\lesssim \int_0^{|n|-1} + \int_{|n|+1}^{\infty}\frac{|n|}{(x+1)(|n|-x)^2}\mathrm{d}x \lesssim 1.$$

Using (4.12), we get

$$
\begin{aligned}
\|\mathrm{diag}A^{-1}\delta A\|_\infty &\leqslant \max_n \left\{ \sum_{k=-N,k\neq n}^{N} |t_{n,n}^{(1)}|(|\hat{a}_{n,k}^{(1)}|+|\hat{a}_{n,k}^{(3)}|) + |t_{n,n}^{(3)}|(|\hat{a}_{n,k}^{(2)}|+|\hat{a}_{n,k}^{(4)}|), \right.\\
&\qquad\qquad \left. \sum_{k=-N,k\neq n}^{N} |t_{n,n}^{(2)}|(|\hat{a}_{n,k}^{(1)}|+|\hat{a}_{n,k}^{(3)}|) + |t_{n,n}^{(4)}|(|\hat{a}_{n,k}^{(2)}|+|\hat{a}_{n,k}^{(4)}|) \right\}\\
&\leqslant \max_n \left(|t_{n,n}^{(1)}|+|t_{n,n}^{(2)}|+|t_{n,n}^{(3)}|+|t_{n,n}^{(4)}| \right) \sum_{k=-N,k\neq n}^{N} \left(|\hat{a}_{n,k}^{(1)}|+|\hat{a}_{n,k}^{(2)}|+|\hat{a}_{n,k}^{(3)}|+|\hat{a}_{n,k}^{(4)}| \right)\\
&\lesssim \max_n \sum_{k=-N,k\neq n}^{N} \left(\frac{\epsilon|n|}{(n-k)^2} + \frac{|n|}{|k|+1}\epsilon \left(\epsilon|n| + \frac{|n|}{(n-k)^2} + \frac{1}{|n-k|^{1/2}} \right) \right)\\
&\lesssim \epsilon N,
\end{aligned}
$$

which, according to the assumption (4.6), yields that

$$
\|\mathrm{diag}A^{-1}\delta A\|_\infty < 1.
$$

Meanwhile, it follows from (4.12) that

$$
\left\| \mathrm{diag}A^{-1} \right\|_\infty \lesssim 1.
$$

Combining the above estimates, we obtain

$$
\|A^{-1}-\mathrm{diag}A^{-1}\|_\infty \leqslant \sum_{k=1}^{\infty} \left\| \mathrm{diag}A^{-1}\delta A \right\|_\infty^k \left\| \mathrm{diag}A^{-1} \right\|_\infty \lesssim \epsilon N.
$$

Hence we derive that

$$
\begin{aligned}
(|n|+1)|C_n-C_{\ell+1,n}| &\leqslant \left\| A^{-1}-\mathrm{diag}A^{-1} \right\|_\infty \|\boldsymbol{b}\|_\infty + |(T^{(2)}\boldsymbol{b}^{(1)}+T^{(4)}\boldsymbol{b}^{(2)})_n|\\
&\lesssim (\epsilon^2+\tau^2+\epsilon\|f-f_N\|_{H^2(0,\Lambda)})(1+|n|)^{1/2}.
\end{aligned}
$$

The error estimate of $\|f_{\ell+1,N}-f\|_{H^2(0,\Lambda)}$ is a consequence of (4.3). $\square$

4.3. Discussion on noisy phase data

In this section, we discuss the estimates when the data is contaminated by some noise. Let $u^\delta(x,h)$ be the noise data such that

$$
\|u^\delta(x,h)-u(x,h)\|_{L^\infty(0,\Lambda)} \leqslant \delta, \tag{4.13}
$$

where $\delta > 0$ is the noise level. Notice that the reconstruction result highly depends on the accuracy of the Rayleigh coefficients in Algorithm 1. We consider the influence of the noise data on Rayleigh's coefficients via formula (3.1). It follows from the assumption $\kappa < 2\pi/\Lambda$ that the noise Rayleigh coefficients A_n^δ satisfy

$$
|A_n^\delta-A_n| \lesssim \mathrm{e}^{|n|h/\Lambda}\delta. \tag{4.14}
$$

If we assume that the cut-off index N satisfies

$$Nh = \mathcal{O}(\Lambda), \tag{4.15}$$

then the difference $|A_n^\delta - A_n|$ between the exact Rayleigh's coefficient and the noise one in the highest frequency mode N is of the order $\mathcal{O}(\delta)$.

Theorem 4.4. *Let the assumptions of theorem 4.3 hold true and the noise data obey (4.13). Then*

$$|C_{\ell+1,n}^\delta - C_n| \lesssim (\epsilon^2 + \tau^2 + \epsilon\|f - f_N\|_{H^2(0,\Lambda)})(1 + |n|)^{-1/2} + \frac{1}{|n|+1}e^{Nh/\Lambda}\delta + e^{|n|h/\Lambda}\delta.$$

Additionally, if the measure height h and the cut-off index N satisfy (4.15), then

$$\|f_{\ell+1,N}^\delta - f\|_{H^2(0,\Lambda)} \lesssim \left(\tau^2 + \epsilon^2 + \delta\right)N^2 + \|f - f_N\|_{H^2(0,\Lambda)}.$$

Proof.   Due to the noise data $u^\delta(x,h)$, an additional term $-2\mathrm{i}\beta_n\Lambda(A_n^\delta - A_n)$ appears in the right hand side of (3.18). The linear system (4.10) and (4.11) is written as

$$\sum_{k=-N}^{N} \hat{a}_{n,k}^{(1)}(B_k - B_k^{(0)} - B_{\ell+1,k}^{(1)}) + \sum_{k=-N,k\neq0}^{N} \hat{a}_{n,k}^{(3)}(|k|+1)(C_k - C_{\ell+1,k}^\delta) = b_n^{(1)},$$

$$\sum_{k=-N,k\neq0}^{N} \hat{a}_{n,k}^{(2)}(B_k - B_k^{(0)} - B_{\ell+1,k}^{(1)}) + \sum_{k=-N,k\neq0}^{N} \hat{a}_{n,k}^{(4)}(|k|+1)(C_k - C_{\ell+1,k}^\delta) = b_n^{(2)} - 2\mathrm{i}\beta_n\Lambda(A_n^\delta - A_n).$$

Let $\tilde{b}_n^{(1)} = b_n^{(1)}$, $\tilde{b}_n^{(2)} = b_n^{(2)} - 2\mathrm{i}\beta_n\Lambda(A_n^\delta - A_n)$, $\boldsymbol{b}^{(j)} = \left(b_{-N}^{(j)}, b_{-N+1}^{(j)}, \ldots, b_N^{(j)}\right)^\top$, and $\tilde{\boldsymbol{b}}^{(j)} = \left(\tilde{b}_{-N}^{(j)}, \tilde{b}_{-N+1}^{(j)}, \ldots, \tilde{b}_N^{(j)}\right)^\top$. From the definition, it follows

$$|\tilde{b}^{(j)}| \lesssim |b^{(j)}| + |\beta_n|e^{|n|h/\Lambda}\delta, \quad \|\tilde{\boldsymbol{b}}^{(j)}\|_\infty \lesssim \|\boldsymbol{b}^{(j)}\|_\infty + \sum_{n=-N}^{N} |\beta_n|e^{|n|h/\Lambda}\delta \lesssim \|\boldsymbol{b}^{(j)}\|_\infty + Ne^{Nh/\Lambda}\delta.$$

We may use the estimate of theorem 4.3 to obtain

$$
\begin{aligned}
(|n|+1)\left|C_n - C_{\ell+1,n}^\delta\right| &\leqslant \left\|A^{-1} - \mathrm{diag}A^{-1}\right\|_\infty \|\tilde{\boldsymbol{b}}\|_\infty + |(T^{(2)}\tilde{\boldsymbol{b}}^{(1)} + T^{(4)}\tilde{\boldsymbol{b}}^{(2)})_n| \\
&\lesssim \left\|A^{-1} - \mathrm{diag}A^{-1}\right\|_\infty \|\boldsymbol{b}\|_\infty + |b_n^{(1)}| + |b_n^{(2)}| + \epsilon N^2 e^{Nh/\Lambda}\delta + (|n|+1)e^{|n|h/\Lambda}\delta \\
&\lesssim (\epsilon^2 + \tau^2 + \epsilon\|f - f_N\|_{H^2(0,\Lambda)})(1+|n|)^{1/2} + e^{Nh/\Lambda}\delta + (|n|+1)e^{|n|h/\Lambda}\delta.
\end{aligned}
$$

The estimate of $\|f_{\ell+1,N}^\delta - f\|_{H^2(0,\Lambda)}$ is followed from (4.3). $\qquad\square$

We point out that the cut-off index N in theorem 4.4 is chosen such that

$$N = \min\left\{N_1, N_2 : \epsilon N_1^2 = \mathcal{O}(1), \ N_2 h = \mathcal{O}(\Lambda)\right\}.$$

The index N_1 is chosen to guarantee the convergence of Algorithm 1. The index N_2 is used to stabilize the measurement error and is usually smaller than N_1. The error between the final approximated surface and the exact surface contains following components:

$$\|f - f_{L,N}^\delta\|_{H^2(0,\Lambda)} \leqslant (\epsilon^2 + \delta)N^2 + \|f - f_N\|_{H^2(0,\Lambda)}.$$

If we choose a small cut-off index N, the truncation error $\|f - f_N\|_{H^2(0,\Lambda)}$ may dominate the total error. On the other hand, if we choose a large cut-off index N, then the condition (4.15) may not be satisfied and the approximated surface may blow up because the noise is exponentially amplified in (4.14). The convergence rate of our proposed Algorithm 1 depends on several aspects, such as the decaying properties of the truncation error $\|f - f_N\|_{H^2(0,\Lambda)}$, where an assumption of higher regularity of f is required, and the balance errors in theorems 4.3 and 4.4.

5. Numerical experiments

In this section, we present some numerical experiments to illustrate our proposed algorithm for both phase and phaseless data. In all experiments, we take the wavenumber $\kappa = \pi/\Lambda$, which yields $\lambda = 2\Lambda$, i.e. the wavelength of incident wave is twice of the surface period. The conventional far-field optics cannot capture the details of the surface by using this incident field due to the diffraction limit. As is shown below, our proposed algorithm can break the diffraction limit and obtain subwavelength resolution. Theoretically, the assumptions $\|f\|_{H^2(0,\Lambda)} < \epsilon$ and $\epsilon N^2 = \mathcal{O}(1)$ are needed in the proof of theorem 4.3. In practice, the assumption can be released to

$$\max_x |f(x)| N^{3/2} \leqslant \Lambda \tag{5.1}$$

for noise free data and

$$N = \min \left\{ N_1, N_2 : \max_x |f(x)| N_1^{3/2} \leqslant \Lambda, \ N_2 h \leqslant \Lambda \right\} \tag{5.2}$$

for the noise data with phase information.

The results in theorems 4.3 and 4.4 show that any initial guess $\|f_0\|_{H^2(0,\Lambda)} \leqslant \epsilon$ yields the convergence, which is verified by our numerical experience. Moreover, the smaller τ (satisfying $\|f_0 - f\| \leqslant \tau$) is, the less iteration is needed. Noting that the exact surface is a small perturbation from the flat surface, we simply choose the initial guess in all examples as $f_0 = 0$.

5.1. Reconstruction with phase data

First we consider noise free phase data. In this case, the error depends only on the deformation constant ϵ and the cut-off index N, whereas the measure height h has no impact. We illustrate this conclusion in the following examples.

Example 5.1.   The exact surface function is

$$f(x) = M(\cos(x) + \cos(5x) + \cos(10x) - 3),$$

where we consider different parameters:

 (i) $M = 0.05$, the cut-off index $N = 10$, the measure height $h = 0.1\lambda$;
 (ii) $M = 0.2$, the cut-off index $N = 10$, the measure height $h = 0.01\lambda$;
(iii) $M = 0.05$, the cut-off index $N = 10$, the measure height $h = 0.01\lambda$;
(iv) $M = 0.05$, the cut-off index $N = 9$, the measure height $h = 0.01\lambda$.

It can be verified that the condition (5.1) is satisfied in each case. The numerical results are shown in figure 3. The following observations can be made:
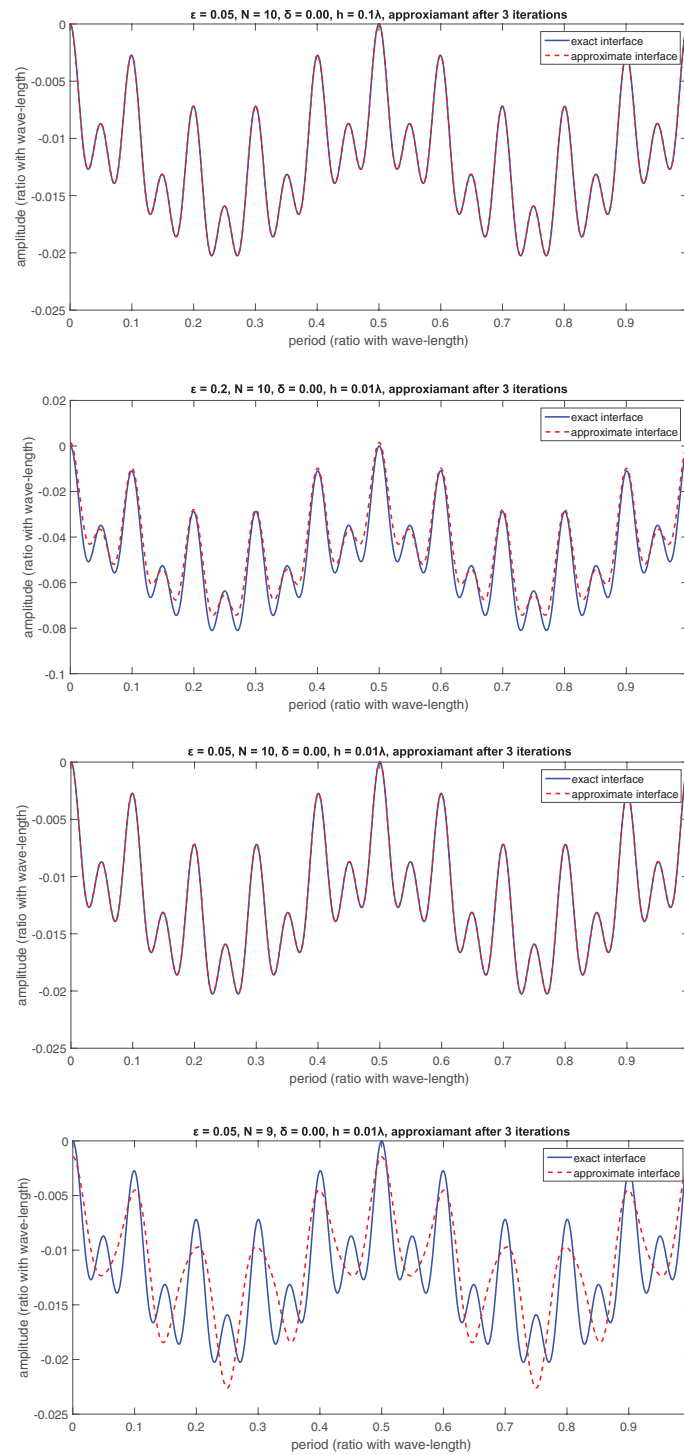
Figure 3. Example 5.1 (noise free data). Reconstructed surfaces are plotted against the exact surface. From top to bottom: (a) case (i); (b) case (ii); (c) case (iii); (d) case (iv). The number of iterations $L = 3$.
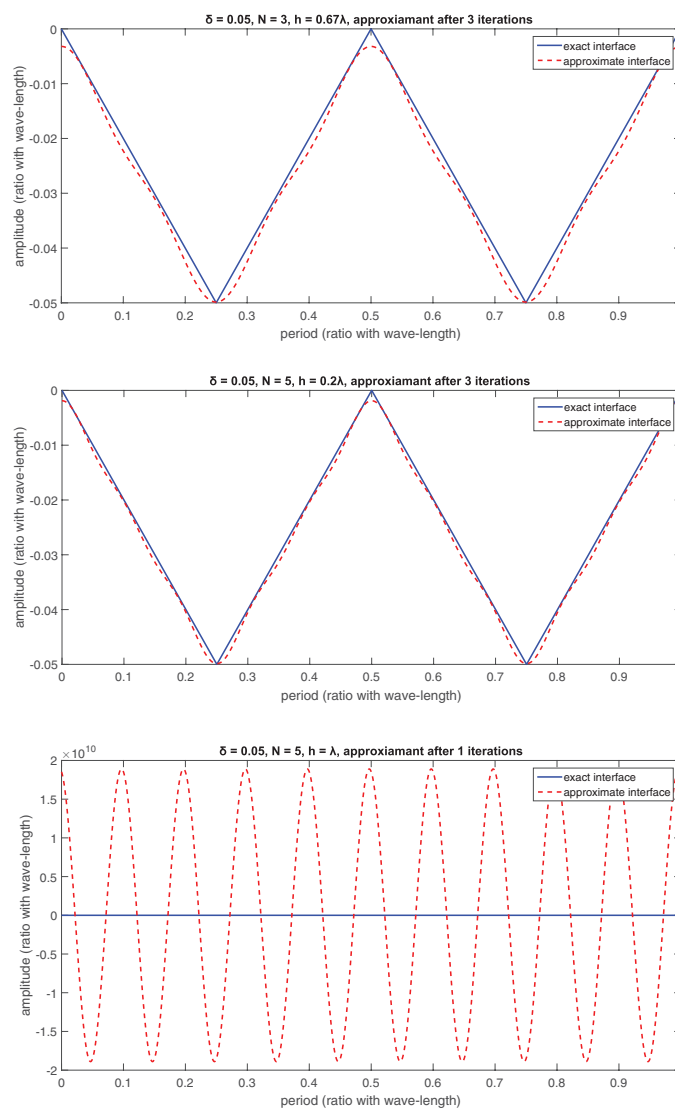
Figure 4. Example 5.2 (noise data). Reconstructed surfaces are plotted against the exact one. From top to bottom: (a) case (i) $N = 3$, $h = 0.67\lambda$, $L = 3$; (b) case (ii) $N = 5$, $h = 0.2\lambda$, $L = 3$; (c) case (iii) $N = 5$, $h = \lambda$, $L = 1$.

(1) Comparison of (i) and (iii): in both cases, the difference is the measure height h which, as we have discussed above, has no impact on the error estimate if (5.1) is satisfied. Although the case (iii) has a ten times smaller measure height than the case (i), the reconstructions are of the same accuracy.

(2) Comparison of (ii) and (iii): the difference between case (ii) and (iii) is the deformation parameter ϵ. By taking the same cut-off index $N = 10$, figure 3(c) shows a better reconstruction than figure 3(b) does.
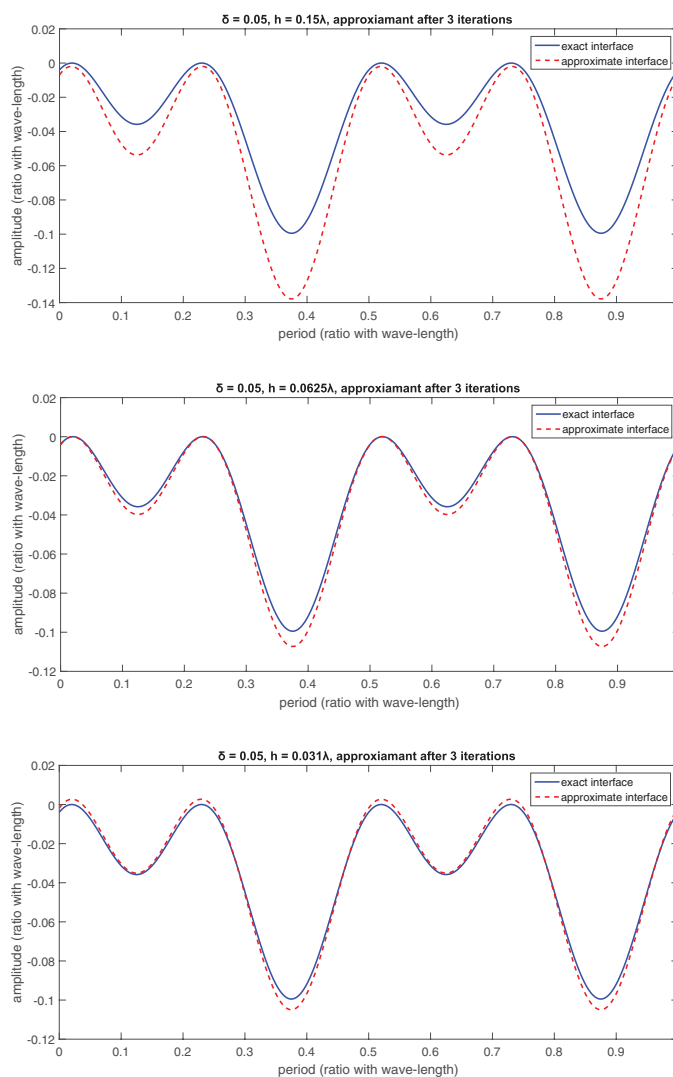
Figure 5. Example 5.3 (noise phaseless data). Reconstructed surfaces are plotted against the exact one. (a) case (i) $h = 0.15\lambda$, $N = 2$, $L = 3$; (b) case (ii) $h = 0.0625\lambda$, $N = 2$, $L = 3$; (c) case (iii) $h = 0.031\lambda$, $N = 2$, $L = 3$.

(3) Comparison of (iii) and (iv): the cases of (iii) and (iv) have different cut-off parameters N. We note that the chosen N in the case (iv) does not cover all the frequency modes in the surface function. Hence the reconstruction loses small fine structures, whereas the reconstruction in the case (iii) has fully recovered the surface function.

Example 5.2.　In this example, we consider noise data. The exact surface function is

$$f(x) = 0.2 \left(\left| \frac{x}{2\pi} - \pi \right| - \pi \right). \tag{5.3}$$

The surface (5.3) is a nonsmooth function and it has infinitely many Fourier modes. We consider three different cases:

  (i) the cut-off index $N = 3$ and the measurement height $h = 0.67\lambda$;
 (ii) the cut-off index $N = 5$ and the measurement height $h = 0.2\lambda$;
(iii) the cut-off index $N = 5$ and the measurement height $h = \lambda$.

The results are shown in figure 4. We observe that: the case (iii) does not satisfy the requirement (5.2) which is important to obtain a stable recovery; The reconstructed surfaces are quite accurate if the cut-off index N satisfies (5.2); As long as the truncation error dominates the overall error, the larger the cut-off N is, the finer the recovered surface function is; if (5.2) is not satisfied, the reconstructed surface blows up immediately after the first iteration.

5.2. Reconstructions with phaseless data

Now we consider phaseless noise data. As shown in (4.15), the following heuristic condition is used to determine the measure height:

$$Nh \leqslant \frac{\Lambda}{4}. \tag{5.4}$$

We focus on the consequence of changing the measure height h if the above condition is not satisfied.

Example 5.3. The exact surface is

$$f(x) = 0.4(\sin(x) + \cos(2x) - 1.124\,997\,781\,483\,376).$$

We also consider three cases:

  (i) the cut-off index $N = 2$ and the measurement height $h = 0.15\lambda$;
 (ii) the cut-off index $N = 2$ and the measurement height $h = 0.0625\lambda$;
(iii) the cut-off index $N = 2$ and the measurement height $h = 0.031\lambda$,

where case (i) the parameters do not satisfy the condition (5.4).

   Figure 5 shows the reconstructed surfaces by using different h and N given above. Figure 5(a) verifies the importance of the condition (5.4), where some of the main information is lost because of the noise. At the same time, both the height $h = 0.0625\lambda$ and $h = 0.031\lambda$ provide reasonable reconstructions but the latter is more accurate due to the smaller dropping terms in (3.3)–(3.7) when we recover Rayleigh's coefficients for the phaseless data.

6. Conclusion

We have presented a novel computational method for the inverse diffraction grating problem. The surface is assumed to be a sufficiently smooth and small perturbation from the flat surface. Subwavelength resolution is achieved by using the phase or phaseless data. Monotonicity is proved for the error estimate between the exact surface and the reconstructed surface. Numerical results show that the method is effective to reconstruct the grating surfaces with super-resolved resolution. By calibrating the Rayleigh expansion carefully, our proposed approach also works for the sound-hard and impedance surfaces. We are currently extending the method to the biperiodic structures, where the three-dimensional Maxwell equations need to be considered. The results will be reported elsewhere.

Acknowledgments

Appendix A. Useful formulas and proof of lemmas

We present derivation of several useful formulas below which are referred in the context.

A.1. Derivation of the formula (3.3)–(3.7)

Multiplying (2.3) by its complex conjugate, we obtain

$$|u(x,h)|^2 = 1 + \sum_{n \in \mathbb{Z}} \left(A_n e^{i(\alpha_n x + (\kappa + \beta_n)h)} + \bar{A}_n e^{-i(\alpha_n x + (\kappa + \bar{\beta}_n)h)} \right)$$
$$+ \sum_{n,m \in \mathbb{Z}} A_n \bar{A}_m e^{i(\alpha_{n-m} x + (\beta_n - \bar{\beta}_m)h)}. \tag{A.1}$$

Comparing the Fourier coefficients on both sides of (A.1) and noticing $\beta_m = \beta_{-m}$, we can obtain

$$\frac{1}{\Lambda} \int_0^{\Lambda} |u(x,h)|^2 e^{i\alpha_m x} dx - \delta_{0m} = A_{-m} e^{i(\kappa + \beta_m)h} + \bar{A}_m e^{-i(\kappa + \bar{\beta}_m)h}$$
$$+ \sum_{n \in \mathbb{Z}} A_n \bar{A}_{n+m} e^{i(\beta_n - \bar{\beta}_{m+n})h}. \tag{A.2}$$

Recalling that f is a small perturbation of the flat surface, we have that

$$|A_0| = \mathcal{O}(1), \quad |A_n| = \mathcal{O}(\epsilon),\ n \neq 0.$$

Dropping $\mathcal{O}(\epsilon^2)$ terms in (A.2), we obtain approximated nonlinear equations:

$$\frac{1}{\Lambda} \int_0^{\Lambda} |u(x,h)|^2 dx - 1 = A_0 e^{2i\kappa h} + \bar{A}_0 e^{-2i\kappa h} + |A_0|^2 \tag{A.3}$$

and

$$\frac{1}{\Lambda} \int_0^{\Lambda} |u(x,h)|^2 e^{i\alpha_m x} dx = \left(e^{i(\kappa + \beta_m)h} + \bar{A}_0 e^{i(-\kappa + \beta_m)h} \right) A_{-m}$$
$$+ \left(e^{-i(\kappa + \bar{\beta}_m)h} + A_0 e^{i(\kappa - \bar{\beta}_m)h} \right) \bar{A}_m. \tag{A.4}$$

Then, with the additional condition (3.2), we obtain (3.3) and (3.4) by combining $|A_0| = 1$ with (A.3) and letting $A_0 = \text{Re}A_0 + i\text{Im}A_0$:

$$(\text{Re}A_0)^2 + (\text{Im}A_0)^2 = 1,$$
$$\frac{1}{2\Lambda} \int_0^{\Lambda} |u(x,h)|^2 dx - 1 = \cos(2\kappa h)\text{Re}A_0 - \sin(2\kappa h)\text{Im}A_0,$$

which has a unique solution if we seek the solution around -1 for $\mathrm{Re}A_0$. After retrieving A_0, we use the fact that $|A_m| = |A_{-m}|$ and let

$$A_m = r_m \mathrm{e}^{\mathrm{i}\theta_m} = r_m \sin\theta_m + \mathrm{i}r_m \cos\theta_m,$$

$$A_{-m} = r_m \mathrm{e}^{\mathrm{i}\varphi_m} = r_m \sin\varphi_m + \mathrm{i}r_m \cos\varphi_m.$$

Plugging the above expressions into (A.4), we obtain after a straightforward calculation that

$$2r_m \cos\left(\frac{\theta_m - \varphi_m}{2}\right) \left(\mathrm{Im}(C_m)\cos\left(\frac{\theta_m + \varphi_m}{2}\right) + \mathrm{Re}(C_m)\sin\left(\frac{\theta_m + \varphi_m}{2}\right)\right)$$
$$= \mathrm{Re}\left(\frac{1}{\Lambda}\int_0^\Lambda |u(x,h)|^2 \mathrm{e}^{\mathrm{i}\alpha_m x}\mathrm{d}x\right)$$

and

$$2r_m \sin\left(\frac{\theta_m - \varphi_m}{2}\right) \left(\mathrm{Im}(C_m)\cos\left(\frac{\theta_m + \varphi_m}{2}\right) + \mathrm{Re}(C_m)\sin\left(\frac{\theta_m + \varphi_m}{2}\right)\right)$$
$$= \mathrm{Im}\left(\frac{1}{\Lambda}\int_0^\Lambda |u(x,h)|^2 \mathrm{e}^{\mathrm{i}\alpha_m x}\mathrm{d}x\right),$$

where

$$C_m = \mathrm{e}^{-\mathrm{i}(\kappa + \bar{\beta}_m)h} + A_0 \mathrm{e}^{\mathrm{i}(\kappa - \bar{\beta}_m)h}.$$

Consequently, the phase difference $\theta_m - \varphi_m := \Phi(m)$ satisfies

$$\tan\left(\frac{\theta_m - \varphi_m}{2}\right) = \mathrm{Im}\left(\int_0^\Lambda |u(x,h)|^2 \mathrm{e}^{\mathrm{i}\alpha_m x}\mathrm{d}x\right) \Big/ \mathrm{Re}\left(\int_0^\Lambda |u(x,h)|^2 \mathrm{e}^{\mathrm{i}\alpha_m x}\mathrm{d}x\right),$$

which provides the relationship between A_m and A_{-m} as in (3.5) and (3.6).

A.2. Proof of lemmas

Proof of lemma 4.1.   Noting that

$$\partial_{\nu_j} u_j = (1 + (f_j')^2)^{-1/2}\left(f_j' \partial_x u_1(x, f_j) - \partial_y u_j(x, f_j)\right),$$

we have

$$\|(1 + (f_1')^2)^{1/2}\partial_{\nu_1} u_1 - (1 + (f_2')^2)^{1/2}\partial_{\nu_2} u_2\|_{H^{1/2}(0,\Lambda)}$$
$$\leqslant \|f_1' \partial_x(u_1(x,f_1) - u_2(x,f_2)) - (f_2' - f_1')\partial_x u_2(x,f_2) - \partial_y(u_1(x,f_1) - u_2(x,f_2))\|_{H^{1/2}(0,\Lambda)}$$
$$\lesssim \|u_1(x,f_1) - u_2(x,f_2)\|_{H^{3/2}(0,\Lambda)} + \tau.$$

It requires to estimate $\|u_1(x,f_1) - u_2(x,f_2)\|_{H^{3/2}(0,\Lambda)}$ in order to prove the error estimate.

Recall that u_j satisfies the boundary value problem:

$$\begin{cases} \Delta u_j + \kappa^2 u_j = 0 & \text{in } \Omega_j, \\ u_j = 0 & \text{on } \Gamma_{f_j}, \\ \partial_y u_j = T u_j - 2\mathrm{i}\kappa \mathrm{e}^{-\mathrm{i}\kappa} & \text{on } \Gamma_1. \end{cases}$$

Consider the transformation

$$\tilde{x} = x, \quad \tilde{y} = \left(\frac{1-f_1}{1-f_2}\right) y + \left(\frac{f_1-f_2}{1-f_2}\right), \quad x \in [0, \Lambda], \ y \in [f_2(x), 1], \tag{A.5}$$

which transforms the sub-domain Ω_2 into Ω_1.

Let ω be the transformed function of u_2 under (A.5). Dropping the tilde for simplicity of notation, we derive

$$\begin{cases} \partial_{xx}\omega + c_1\partial_{yy}\omega + c_2\partial_{xy}\omega + c_3\partial_y\omega + \kappa^2\omega = 0 & \text{in } \Omega_1, \\ \omega = 0 & \text{on } \Gamma_{f_1}, \\ \partial_y\omega = (T\omega - 2i\kappa e^{-i\kappa})(1 + (f_1-f_2)/(1-f_1)) & \text{on } \Gamma_1, \end{cases}$$

where

$$c_1 = \left((1-f_1)^2(1-f_2)^2 + (1-y)^2\left((1-f_1)(f_1'-f_2') + f_1'(f_1-f_2)\right)^2\right)/(1-f_2)^4,$$

$$c_2 = \left(2(1-y)\left((1-f_1)(f_1'-f_2') + f_1'(f_1-f_2)\right)\right)/(1-f_2)^2,$$

$$c_3 = \left((1-y)\left(2(f_2')^2(f_1-f_2) + (1-f_2)\left((1-f_1)(f_1''-f_2'')\right.\right.\right.$$
$$\left.\left.\left. + f_1''(f_1-f_2) + 2f_2'(f_1'-f_2')\right)\right)\right)/(1-f_2)^3\right).$$

Let $p = u_1 - \omega$. It is easy to note that

$$\begin{cases} \Delta p + \kappa^2 p = g & \text{in } \Omega_1, \\ p = 0 & \text{on } \Gamma_{f_1}, \\ \partial_y p = Tp + \varphi & \text{on } \Gamma_1, \end{cases}$$

where

$$g = (1-c_1)\partial_{yy}\omega - c_2\partial_{xy}\omega - c_3\partial_y\omega, \quad \varphi = (T\omega - 2i\kappa e^{-i\kappa})(f_1-f_2)/(1-f_1).$$

It follows from the regularity of surface functions f_j and the condition $f_j \leqslant 0$ that

$$\left|\frac{1}{1-f_j}\right| \lesssim 1, \quad |1-f_j| \lesssim 1, \quad \|f_1''-f_2''\|_{L^4(0,\Lambda)} \lesssim \|f_1''-f_2''\|_{L^2(0,\Lambda)}.$$

Combining the above inequalities with (4.4), we have from the Hölder inequality that

$$\|1-c_1\|_{L^\infty(\Omega_1)}$$
$$= \left\|\frac{(1-f_2)^2(2-f_1-f_2)(f_2-f_1) - (1-y)^2\left((1-f_1)(f_1'-f_2') + f_1'(f_1-f_2)\right)^2}{(1-f_2)^4}\right\|_{L^\infty(\Omega_1)}$$
$$\lesssim \|(2-f_1-f_2)(f_2-f_1)\|_{L^\infty(\Omega_1)} + \|\left((1-f_1)(f_1'-f_2') + f_1'(f_1-f_2)\right)^2\|_{L^\infty(\Omega_1)}$$
$$\lesssim \|f_2-f_1\|_{L^\infty(\Omega_1)} + \|(f_1'-f_2')^2 + (f_1-f_2)^2 + (f_1'-f_2')(f_1-f_2)\|_{L^\infty(\Omega_1)} \lesssim \tau$$

and

$$\|c_2\|_{L^\infty(\Omega_1)} \lesssim \|(1-f_1)(f_1'-f_2')\|_{L^\infty(\Omega_1)} + \|f_1'(f_1-f_2)\|_{L^\infty(\Omega_1)} \lesssim \tau,$$
$$\|c_3\|_{L^4(\Omega_1)} \lesssim \|f_1-f_2\|_{L^4(\Omega_1)} + \|f_1''-f_2''\|_{L^4(\Omega_1)} + \|f_1'-f_2'\|_{L^4(\Omega_1)} \lesssim \tau.$$

It follows from the well-posedness of the boundary value problem for w that

$$\|\omega\|_{H^2(\Omega_1)} \lesssim 1.$$

Applying the Sobolev imbedding theorem yields that

$$\|g\|_{L^2(\Omega_1)} \leqslant \left(\|1 - c_1\|_{L^\infty(\Omega_1)} + \|c_2\|_{L^\infty(\Omega_1)} + \|c_3\|_{L^4(\Omega_1)} \right) \|\omega\|_{H^2(\Omega_1)} \lesssim \tau. \tag{A.6}$$

On the other hand, since the operator T is a bounded operator, it implies that

$$\|\varphi\|_{H^{1/2}(\Gamma_1)} \lesssim \tau. \tag{A.7}$$

Using (A.6) and (A.7) and the classical result of elliptic equations (see [25]), we obtain

$$\|p\|_{H^2(\Omega_1)} \lesssim \|g\|_{L^2(\Omega_1)} + \|\varphi\|_{H^{1/2}(\Gamma_1)} \lesssim \tau.$$

Following the trace theorem it yields

$$\|u_1(x,f_1) - u_2(x,f_2)\|_{H^{3/2}(0,\Lambda)} = \|u_1(x,f_1) - \omega(x,f_1)\|_{H^{3/2}(0,\Lambda)} \lesssim \|p\|_{H^2(\Omega_1)} \lesssim \tau,$$

which completes the proof. □

Proof of lemma 4.2.　Recall that the coefficients $B_{m,N}$ satisfies

$$\sum_{m=-\infty}^{\infty} \left(\int_0^\Lambda e^{i(\alpha_{m-n}x + \beta_n f_{\ell,N}(x))} \mathrm{d}x \right) B_{m,N} = 2i\kappa\Lambda\delta_{0n}, \quad n = 0, \pm1, \dots, \pm N.$$

Using (3.16), we obtain for $m = 0, \pm1, \dots, \pm N$ that

$$\sum_{m=-N}^{N} \left(\int_0^\Lambda e^{i(\alpha_{m-n}x + \beta_n f_{\ell,N}(x))} \mathrm{d}x \right) (B_{m,N} - B_m^{(0)})$$

$$= -\sum_{|m|>N} \left(\int_0^\Lambda e^{i(\alpha_{m-n}x + \beta_n f_{\ell,N}(x))} \mathrm{d}x \right) B_{m,N}, \quad n = 0, \pm1, \dots, \pm N. \tag{A.8}$$

Denote

$$a_{n,m} = \int_0^\Lambda e^{i(\alpha_{m-n}x + \beta_n f_{\ell,N}(x))} \mathrm{d}x, \quad x_m = B_{m,N} - B_m^{(0)}, \quad y_n = -\sum_{|m|>N} a_{n,m} B_{m,N}.$$

The linear system (A.8) can be reformulated into the matrix form:

$$A\boldsymbol{x} = \boldsymbol{y}, \tag{A.9}$$

where $\boldsymbol{x} = (x_{-N}, x_{-N+1}, \dots, x_N)^\top, \boldsymbol{y} = (y_{-N}, y_{-N+1}, \dots, y_N)^\top$, and

$$A = \begin{pmatrix} a_{-N,-N} & a_{-N,-N+1} & \cdots & a_{-N,N} \\ a_{-N+1,-N} & a_{-N+1,-N+1} & \cdots & a_{-N+1,N} \\ \vdots & \vdots & \ddots & \vdots \\ a_{N,-N} & a_{N,-N+1} & \cdots & a_{N,N} \end{pmatrix}.$$

It is required to estimate $B_{m,N} - B_m^{(0)} = x_m = (A^{-1}\boldsymbol{y})_m, m = 0, \pm 1, \dots, \pm N$.

Let $A = A_1 + A_2$, where

$$
A_1 = \begin{pmatrix} a_{-N,-N} & 0 & \dots & 0 \\ 0 & a_{-N+1,-N+1} & \dots & 0 \\ \vdots & \vdots & \ddots & \vdots \\ 0 & 0 & \dots & a_{N,N} \end{pmatrix}, \quad A_2 = \begin{pmatrix} 0 & a_{-N,-N+1} & \dots & a_{-N,N} \\ a_{-N+1,-N} & 0 & \dots & a_{-N+1,N} \\ \vdots & \vdots & \ddots & \vdots \\ a_{N,-N} & a_{N,-N+1} & \dots & 0 \end{pmatrix}.
$$

It is easy to verify that the matrix A is strongly diagonally dominant. Using lemma B.1 and the assumption (4.5), we have

$$
\begin{aligned}
\|A_1^{-1}A_2\|_\infty &= \max_n \sum_{m=-N,m\neq n}^{N} |a_{n,m}/a_{n,n}| \\
&\leqslant \max_n \sum_{m=-N,m\neq n}^{N} \frac{18\epsilon|\beta_n|}{\Lambda(m-n)^2} \leqslant \frac{6\pi^2}{\Lambda}\epsilon \max_n |\beta_n| < 1,
\end{aligned}
$$

which yields

$$
(I + A_1^{-1}A_2)^{-1} = \sum_{k=0}^{\infty}(-A_1^{-1}A_2)^k.
$$

Hence we have

$$
\left\|A^{-1} - A_1^{-1}\right\|_\infty \leqslant \sum_{k=1}^{\infty}\left\|A_1^{-1}A_2\right\|_\infty^k \left\|A_1^{-1}\right\|_\infty \lesssim \epsilon \max_n |\beta_n|.
$$

Next, we estimate y_n in (A.9). It is easy to note that

$$
|y_n| \leqslant \left|\sum_{|m|\geqslant N} a_{n,m}(B_{m,N} - B_m^{f_0})\right| + \left|\sum_{|m|\geqslant N} a_{n,m}B_m^{f_0}\right|
$$

with $f_0(x) = 0$ and

$$
\partial_\nu u(x,f_0(x)) = \sum_{m\in\mathbb{Z}} B_m^{f_0}e^{i\alpha_m x}, \quad B_m^{f_0} \in \mathbb{C}.
$$

Noting that $f_{\ell,N}(x)$ and $f_0(x) = 0$ satisfy the assumptions of lemma 4.1 with $\tau = \epsilon$, we obtain

$$
\left\|(1 + (f_{\ell,N}')^2)^{1/2}\partial_{\nu_{f_{\ell,N}}}u - \partial_{\nu_{f_0}}u_0\right\|_{H^{1/2}(0,\Lambda)} \lesssim \epsilon.
$$

Choosing $f_0(x) = 0$, we obtain $u_0(x,y) = e^{-i\kappa y} - e^{i\kappa y}$ and $\partial_{\nu_{f_0}}u_0 = -2i\kappa$. If $F(x) \in H^{1/2}(0,\Lambda)$, it follows from the decay rate of Fourier coefficients in [26] that the Fourier coefficient $\widehat{F}(n)$ satisfies

$$
|\widehat{F}(n)| \lesssim |n|^{-1/2}\|F\|_{H^{1/2}(0,\Lambda)} \quad \text{for } n \neq 0.
$$

In particular, the Fourier coefficient of $\partial_{\nu_{f_0}} u_0$ satisfies

$$\widehat{\partial_{\nu_{f_0}} u_0}(m) = \begin{cases} 0 & \text{for } m \neq 0, \\ -2i\kappa\Lambda & \text{for } m = 0, \end{cases}$$

which yields

$$\begin{cases} |B_{m,N}| \lesssim \epsilon|m|^{-1/2} & \text{for } m \neq 0, \\ |B_{m,N} + 2i\kappa\Lambda| \lesssim \epsilon & \text{for } m = 0. \end{cases} \tag{A.10}$$

It follows from the above discussion that

$$|y_n| \lesssim \sum_{|m|>N} \frac{\epsilon^2|\beta_n|}{|m|^{1/2}(m-n)^2} \lesssim \frac{\epsilon^2|\beta_n|}{N^{1/2}}.$$

Combining the above estimates, we obtain

$$\begin{aligned} |B_{m,N} - B_m^{(0)}| &\leqslant |(A_1^{-1}y)_m| + \left\|A^{-1} - A_1^{-1}\right\|_\infty \|y\|_\infty \\ &\lesssim \epsilon^2|\beta_m|N^{-1/2} + \epsilon^3 N^{-1/2} \max_n |\beta_n|^2 \\ &\lesssim \epsilon^2 N^{-1/2} \max_n |\beta_n|, \end{aligned}$$

which complete the proof. $\qquad\qquad\square$

Appendix B. Technical lemmas

In this section, we provide detailed estimates used in proof of theorem 4.3.

Lemma B.1.   *Let $f_{\ell,N}$ be a surface function satisfying*

$$\|f_{\ell,N}\|_{H^2(0,\Lambda)} < \frac{\epsilon}{\max\{\sqrt{\Lambda}, 1/\sqrt{\Lambda}\}}.$$

If the deformation parameter ϵ is small enough such that

$$\epsilon \max_n |\beta_n| < 1.$$

Then the variables $a_{n,m}^{(j)}$ defined by

$$a_{n,m}^{(j)} = \int_0^\Lambda e^{i(\alpha_{m-n}x + (-1)^{j+1}\beta_n f_{\ell,N})}\mathrm{d}x, \quad j = 1, 2$$

admit the following error estimates:

$$|a_{n,m}^{(j)}| \leqslant \frac{6\epsilon|\beta_n|}{(n-m)^2} \text{ for } n \neq m, \quad \frac{1}{3}\Lambda \leqslant |a_{n,m}^{(j)}| \leqslant 3\Lambda \text{ for } n = m.$$

Proof.   For simplicity's sake, we only show the estimate for $a_{n,m}^{(1)}$ since the proof for $a_{n,m}^{(2)}$ is similar. Using the classical results of Fourier analysis in [26] and noting

$$\left|e^{i\beta_n f_{\ell,N}(x)}\right| \leqslant e^{|\beta_n f_{\ell,N}(x)|} \leqslant e^{\epsilon|\beta_n|} \leqslant e < 3,$$

we have

$$
\begin{aligned}
|a_{n,m}^{(1)}| = \left| \widehat{e^{i\beta_n f_{\ell,N}(x)}}(n-m) \right| &\leqslant \frac{1}{(n-m)^2} \left\| (e^{i\beta_n f_{\ell,N}(x)})'' \right\|_{L^1(0,\Lambda)} \\
&\leqslant \frac{3\sqrt{\Lambda}|\beta_n|}{(n-m)^2} \left\| f_{\ell,N}''(x) + (f_{\ell,N}'(x))^2 \beta_n \right\|_{L^2(0,\Lambda)} \\
&\leqslant \frac{6\epsilon|\beta_n|}{(n-m)^2},
\end{aligned}
$$

where we have used the smallness assumption of $\|f_{\ell,N}\|_{H^2(0,\Lambda)}$ and $\max_n \epsilon|\beta_n| < 1$.

It follows from (2.4) that β_n is a positive real number if $n \leqslant \Lambda/\lambda$. We can decompose

$$
e^{i\beta_n f_{\ell,N}(x)} = \cos(\beta_n f_{\ell,N}(x)) + i\sin(\beta_n f_{\ell,N}(x)).
$$

Noting that $0 \geqslant \beta_n f_{\ell,N}(x) \geqslant -\epsilon|\beta_n| > -\pi/2$, we get

$$
\begin{aligned}
\left| a_{n,n}^{(1)} \right| &= \left| \int_0^\Lambda \cos(\beta_n f_{\ell,N}(x)) + i\sin(\beta_n f_{\ell,N}(x)) \, dx \right| \\
&= \left(\left| \int_0^\Lambda \cos(\beta_n f_{\ell,N}(x)) \, dx \right|^2 + \left| \int_0^\Lambda \sin(\beta_n f_{\ell,N}(x)) \, dx \right|^2 \right)^{1/2} \\
&\geqslant \left| \int_0^\Lambda \cos(-\epsilon|\beta_n|) \, dx \right| = \Lambda \cos(-\epsilon|\beta_n|).
\end{aligned}
$$

On the other hand, $e^{i\beta_n f_{\ell,N}(x)}$ is a positive real number if $n > \Lambda/\lambda$. A straightforward calculation yields

$$
\left| a_{n,n}^{(1)} \right| \geqslant \Lambda \min_{x \in [0,\Lambda]} e^{i\beta_n f_{\ell,N}(x)} \geqslant \Lambda e^{-\epsilon|\beta_n|}.
$$

Since $e^x \leqslant \cos(x)$ when $-1 \leqslant x \leqslant 0$, we combine both lower bounds and have

$$
\left| a_{n,n}^{(1)} \right| \geqslant \Lambda e^{-\epsilon|\beta_n|} \geqslant \frac{1}{3}\Lambda \text{ for } n = 0, \pm 1, \ldots, \pm N.
$$

The upper bound is easily shown as follows

$$
|a_{n,n}^{(1)}| \leqslant \Lambda \max |e^{i\beta_n f_{\ell,N}(x)}| \leqslant 3\Lambda.
$$

Lemma B.2. *Let $f_{\ell,N}$ be a surface function satisfying*

$$
\|f_{\ell,N}\|_{H^2(0,\Lambda)} < \frac{\epsilon}{\max\{\sqrt{\Lambda}, 1/\sqrt{\Lambda}\}}, \quad (1 + (f_{\ell,N}')^2)^{1/2} \partial_\nu u = \sum_{m \in \mathbb{Z}} B_m e^{i\alpha_m x}.
$$

Let $B_n^{(0)}$ be the coefficient computed in (3.16). If the deformation parameter ϵ is small enough such that

$$
\epsilon \max_n |\beta_n| < 1,
$$

then the variables $\hat{a}_{n,k}^{(j)}$ defined as

27

$$\hat{a}_{n,k}^{(j)} = (-1)^{j+1}\mathrm{i}\frac{\beta_n}{|k|+1}\sum_{m=-N}^{N}B_m^{(0)}\int_0^{\Lambda}\mathrm{e}^{\mathrm{i}(\alpha_{k-n+m}+(-1)^{j+1}\beta_n f_{\ell N})}\mathrm{d}x, \quad j=3,4$$

admit the following error estimates:

$$\begin{cases} |\hat{a}_{n,k}^{(j)}| \lesssim \frac{|\beta_n|}{|k|+1}\epsilon\left(\epsilon|\beta_n| + \frac{|\beta_n|}{(n-k)^2} + \frac{1}{|n-k|^{1/2}}\right) & \text{for } n \neq k, \\ |\hat{a}_{n,k}^{(j)}| \lesssim \frac{|\beta_n|}{|n|+1} & \text{for } n = k. \end{cases}$$

Moreover,

$$|\hat{a}_{n,n}^{(4)} - \hat{a}_{n,n}^{(2)}\hat{a}_{n,n}^{(3)}/\hat{a}_{n,n}^{(1)}| \geqslant \frac{|\beta_n|}{(|n|+1)}\left(\frac{4}{3}\kappa\Lambda^2 - C\epsilon|\beta_n|\right),$$

where the constant C is independent on ϵ, h, n.

Proof.   We present the proof for $\hat{a}_{n,k}^{(3)}$ and omit the discussion on $\hat{a}_{n,k}^{(4)}$. First task is to evaluate $B_n^{(0)}$. Noting $\|f_{\ell,N}\|_{H^2(0,\Lambda)} < \frac{\epsilon}{\max\{\sqrt{\Lambda},1/\sqrt{\Lambda}\}}$ and (A.10), we have

$$\begin{cases} |B_n| \lesssim \epsilon|n|^{-1/2} & \text{for } n \neq 0, \\ |B_n + 2\mathrm{i}\kappa\Lambda| \lesssim \epsilon & \text{for } n = 0. \end{cases}$$

It follows from lemma 4.2 that

$$|B_n - B_n^{(0)}| \lesssim \epsilon^2 N^{-1/2}\max_n|\beta_n| \leqslant \epsilon^2 n^{-1/2}\max_n|\beta_n|.$$

Combining the above two bounds and assuming $\max_n \epsilon|\beta_n| < 1$ lead to

$$|B_n^{(0)} + 2\mathrm{i}\kappa\Lambda\delta_{0n}| \leqslant |B_n + 2\mathrm{i}\kappa\Lambda\delta_{0n}| + |B_n - B_n^{(0)}|.$$

More precisely, we have

$$\begin{cases} |B_n^{(0)}| \lesssim \epsilon|n|^{-1/2} & \text{for } 0 < |n| \leqslant N, \\ |B_n^{(0)} + 2\mathrm{i}\kappa\Lambda| \lesssim \epsilon & \text{for } n = 0. \end{cases} \tag{B.1}$$

Using (B.1), we find the upper bound for $\hat{a}_{n,k}^{(3)}$, $n \neq k$:

$$|\hat{a}_{n,k}^{(3)}| \lesssim \frac{1}{|k|+1}\left(\frac{\epsilon|\beta_n|^2}{(n-k)^2} + \frac{|\epsilon\beta_n|}{|n-k|^{1/2}} + \sum_{\substack{m=-N, m \neq 0 \\ m \neq n-k}}^{N}\frac{|\epsilon\beta_n|^2}{(n-k-m)^2|m|^{1/2}}\right)$$

$$\lesssim \frac{|\beta_n|}{|k|+1}\epsilon\left(\frac{|\beta_n|}{(n-k)^2} + \frac{1}{|n-k|^{1/2}} + \epsilon|\beta_n|\right)$$

and the upper bound for $\hat{a}_{n,n}^{(3)}$:

$$|\hat{a}_{n,n}^{(3)}| \lesssim \frac{1}{|n|+1} \left(|\beta_n| + \sum_{m=-N,m\neq 0}^{N} \frac{|\epsilon\beta_n|^2}{m^{5/2}} \right) \lesssim \frac{|\beta_n|}{|n|+1}.$$

Next, we consider the lower bound for $\hat{a}_{n,n}^{(4)} - \hat{a}_{n,n}^{(2)}\hat{a}_{n,n}^{(3)}/\hat{a}_{n,n}^{(1)}$, which admits

$$|\hat{a}_{n,n}^{(4)} - \hat{a}_{n,n}^{(2)}\hat{a}_{n,n}^{(3)}/\hat{a}_{n,n}^{(1)}| \geqslant \left| \hat{a}_{n,n}^{(4)} - \hat{a}_{n,n}^{(3)} \right| - \left| \left(\hat{a}_{n,n}^{(2)}/\hat{a}_{n,n}^{(1)} - 1 \right) \hat{a}_{n,n}^{(3)} \right|.$$

Since $e^z = \sum_{k=0}^{\infty} z^k/k!, \forall z \in \mathbb{C}$, we have

$$1 - e^{-2i\beta_n f_{\ell,N}} = -\sum_{k=1}^{\infty} (-2i\beta_n f_{\ell,N})^k/k!.$$

It follows from lemma B.1 that

$$\begin{aligned}
\left| \hat{a}_{n,n}^{(2)}/\hat{a}_{n,n}^{(1)} - 1 \right| &= \frac{1}{|\hat{a}_{n,n}^{(1)}|}|\hat{a}_{n,n}^{(2)} - \hat{a}_{n,n}^{(1)}| \\
&\leqslant \frac{3}{\Lambda} \left| \int_0^\Lambda e^{i\beta_n f_{\ell,N}} \left(1 - e^{-2i\beta_n f_{\ell,N}} \right) dx \right| \\
&\lesssim |\sum_{k=1}^{\infty} (-2i\beta_n f_{\ell,N})^k/k!| \lesssim \epsilon|\beta_n|.
\end{aligned} \tag{B.2}$$

Meanwhile,

$$\begin{aligned}
|\hat{a}_{n,n}^{(4)} - \hat{a}_{n,n}^{(3)}| &= \frac{|\beta_n|}{|n|+1} \left| B_0^{(0)}(\hat{a}_{n,n}^{(2)} + \hat{a}_{n,n}^{(1)}) + \sum_{m=N,m\neq 0}^{N} B_m^{(0)} \int_0^\Lambda (e^{i\beta_n f_{\ell,N}} + e^{-i\beta_n f_{\ell,N}}) e^{i\alpha_m x} dx \right| \\
&= \frac{|\beta_n|}{|n|+1} \left| -2i\kappa\Lambda(\hat{a}_{n,n}^{(2)} + \hat{a}_{n,n}^{(1)}) + (B_0^{(0)} + 2i\kappa\Lambda)(\hat{a}_{n,n}^{(2)} + \hat{a}_{n,n}^{(1)}) \right. \\
&\quad \left. + \sum_{m=-N,m\neq 0}^{N} B_m^{(0)} \int_0^\Lambda (e^{i\beta_n f_{\ell,N}} + e^{-i\beta_n f_{\ell,N}}) e^{i\alpha_m x} dx \right| \\
&\geqslant \frac{|\beta_n|}{|n|+1} \left(\left| 2i\kappa\Lambda \left(\hat{a}_{n,n}^{(1)} + \hat{a}_{n,n}^{(2)} \right) \right| - \left| \left(B_0^{(0)} + 2i\kappa\Lambda \right) \left(\hat{a}_{n,n}^{(1)} + \hat{a}_{n,n}^{(2)} \right) \right| \right. \\
&\quad \left. - \sum_{m=-N,m\neq 0}^{N} \left| B_m^{(0)} \int_0^\Lambda \left(e^{i\beta_n f_{\ell,N}} + e^{-i\beta_n f_{\ell,N}} \right) e^{i\alpha_m x} dx \right| \right).
\end{aligned}$$

By definition, we obtain

$$\hat{a}_{n,n}^{(1)} + \hat{a}_{n,n}^{(2)} = \begin{cases} 2\int_0^\Lambda \cos(|\beta_n|f_{\ell,N}) dx & \text{when} \quad n \leqslant \frac{\Lambda}{\lambda} \\ \int_0^\Lambda e^{|\beta_n|f_{\ell,N}} + e^{-|\beta_n|f_{\ell,N}} dx & \text{when} \quad n > \frac{\Lambda}{\lambda}. \end{cases}$$

Noting

$$2\int_0^\Lambda \cos(|\beta_n|f_{\ell,N}) dx \geqslant 2\Lambda\cos(-\epsilon|\beta_n|) \geqslant \frac{2}{3}\Lambda$$

and

$$\int_0^\Lambda \mathrm{e}^{|\beta_n|f_{\ell,N}} + \mathrm{e}^{-|\beta_n|f_{\ell,N}}\mathrm{d}x \geqslant 2\int_0^\Lambda \mathrm{e}^{|\beta_n|f_{\ell,N}}\mathrm{d}x \geqslant 2\Lambda\mathrm{e}^{-\epsilon|\beta_n|} \geqslant \frac{2}{3}\Lambda,$$

we obtain

$$\hat{a}_{n,n}^{(1)} + \hat{a}_{n,n}^{(2)} \geqslant \frac{2}{3}\Lambda.$$

Thus we conclude from (B.1) that there exists a constant C such that

$$|\hat{a}_{n,n}^{(4)} - \hat{a}_{n,n}^{(3)}| \geqslant \frac{|\beta_n|}{|n|+1}\left(\frac{4}{3}\kappa\Lambda^2 - C\epsilon\right). \tag{B.3}$$

Combining (B.2) and (B.3), we have the lower bound:

$$|\hat{a}_{n,n}^{(4)} - \hat{a}_{n,n}^{(2)}\hat{a}_{n,n}^{(3)}/\hat{a}_{n,n}^{(1)}| \geqslant \left|\hat{a}_{n,n}^{(4)} - \hat{a}_{n,n}^{(3)}\right| - \left|\left(\hat{a}_{n,n}^{(2)}/\hat{a}_{n,n}^{(1)} - 1\right)\hat{a}_{n,n}^{(3)}\right|$$

$$\geqslant \frac{|\beta_n|}{|n|+1}\left(\frac{4}{3}\kappa\Lambda^2 - C\epsilon|\beta_n|\right),$$

which completes the proof. □

Lemma B.3. *Let conditions in theorem 4.3 hold true. Then, the variables $b_n^{(i)}$, $i=1,2, n=0,\pm1,\ldots,\pm N$ defined in (4.7) admit the following error estimates*

$$|b_n^{(i)}| \lesssim (\epsilon^2 + \tau^2 + \epsilon\|f - f_N\|_{H^2(0,\Lambda)})(1 + |n|)^{1/2}.$$

Proof. We show the estimate for $b_n^{(1)}$. Recall the definition of $b_n^{(1)}$ in (4.7), it is required to estimate

$$\|\mathrm{e}^{\mathrm{i}\beta_n(f-f_{\ell,N})} - 1 - \mathrm{i}\beta_n(f - f_{\ell,N})\|_{H^2(0,\Lambda)}, \quad \left\|\left(\mathrm{e}^{\mathrm{i}\beta_n f_{\ell,N}}(1 + \mathrm{i}\beta_n(f - f_{\ell,N}))\right)''\right\|_{L^2(0,\Lambda)}, \quad |B_m^{(0)} - B_m|.$$

Noting $e^z = \sum_{k=0}^\infty z^k/k!$ in the complex plane, we obtain

$$\left\|\mathrm{e}^{\mathrm{i}\beta_n(f-f_{\ell,N})} - 1 - \mathrm{i}\beta_n(f - f_{\ell,N})\right\|_{L^2(0,\Lambda)} = \left\|\sum_{k=2}^\infty (\mathrm{i}\beta_n(f - f_{\ell,N}))^k/k!\right\|_{L^2(0,\Lambda)} \lesssim \tau^2|\beta_n|^2,$$

$$\left\|\mathrm{e}^{\mathrm{i}\beta_n(f-f_{\ell,N})} - 1 - \mathrm{i}\beta_n(f - f_{\ell,N})\right\|_{H^1(0,\Lambda)} \lesssim \tau^2|\beta_n|^2 + \|\mathrm{i}\beta_n(f - f_{\ell,N})\|_{H^1(0,\Lambda)}$$

$$\times \left\|\sum_{k=1}^\infty (\mathrm{i}\beta_n(f - f_{\ell,N}))^k/k!\right\| \lesssim \tau^2|\beta_n|^2,$$

$$\left\|\mathrm{e}^{\mathrm{i}\beta_n(f-f_{\ell,N})} - 1 - \mathrm{i}\beta_n(f - f_{\ell,N})\right\|_{H^2(0,\Lambda)} \lesssim \tau^2|\beta_n|^2 + \|\mathrm{i}\beta_n(f - f_{\ell,N})\|_{H^2(0,\Lambda)}$$

$$\times \left\|\sum_{k=1}^\infty (\mathrm{i}\beta_n(f - f_{\ell,N}))^k/k!\right\| \lesssim \tau^2|\beta_n|^2,$$

where we have used the estimates $\tau|\beta_n| \lesssim \epsilon|\beta_n| \lesssim 1$.

A straightforward calculation yields

$$\left\| \left(e^{i\beta_n f_{\ell,N}} (1 + i\beta_n(f - f_{\ell,N})) \right)'' \right\|_{L^2(0,\Lambda)}$$

$$\leqslant \|i\beta_n f''_{\ell,N} e^{i\beta_n f_{\ell,N}} (1 + i\beta_n(f - f_{\ell,N}))\|_{L^2(0,\Lambda)} + \|(i\beta_n f'_{\ell,N})^2 e^{i\beta_n f_{\ell,N}} (1 + i\beta_n(f - f_{\ell,N}))\|_{L^2(0,\Lambda)}$$
$$+ 2\|(i\beta_n)^2 f'_{\ell,N} e^{i\beta_n f_{\ell,N}} (f' - f'_{\ell,N})\|_{L^2(0,\Lambda)} + \|i\beta_n e^{i\beta_n f_{\ell,N}} (f'' - f''_{\ell,N})\|_{L^2(0,\Lambda)} \lesssim (\epsilon + \tau)|\beta_n|$$
$$\lesssim \epsilon|\beta_n|.$$

Recall that $B_{m,N}$ are the Fourier coefficients of $(1 + (f'_{\ell,N}(x))^2)^{1/2} \partial_\nu u_\ell(x, f_{\ell,N}(x))$, $B_m^{(0)}$ is computed in (3.16), and B_m are the Fourier coefficients of $(1 + (f')^2)^{1/2} \partial_\nu u_\ell(x, f(x))$. To obtain the estimate of $B_m^{(0)} - B_m$, we consider

$$\left| B_m^{(0)} - B_m \right| \leqslant \left| B_{m,N} - B_m \right| + \left| B_m^{(0)} - B_{m,N} \right|.$$

By lemma 4.1, we have

$$\left\| \frac{\partial u}{\partial n_{f_{\ell,N}}} (1 + (f'_{\ell,N})^2)^{1/2} - \frac{\partial u}{\partial n_f} (1 + (f')^2)^{1/2} \right\|_{H^{1/2}(0,\Lambda)} \lesssim \tau,$$

which yields

$$|B_{m,N} - B_m| \lesssim \begin{cases} \tau & \text{for } m = 0, \\ \tau|m|^{-1/2} & \text{for } m \neq 0. \end{cases}$$

Since $\kappa < 2\pi/\Lambda$, we have $|\beta_n| \sim n$ and

$$\left| B_m^{(0)} - B_m \right| \leqslant \left| B_m^{(0)} - B_m \right| + |B_{m,N} - B_m|$$
$$\lesssim \epsilon^2 N^{-1/2} \max_n |\beta_n| + \begin{cases} \tau & \text{for } m = 0, \\ \tau|m|^{-1/2} & \text{for } m \neq 0 \end{cases}$$
$$\lesssim \epsilon^2 N^{1/2} + \begin{cases} \tau & \text{for } m = 0, \\ \tau|m|^{-1/2} & \text{for } m \neq 0. \end{cases}$$

For the cases $n \neq 0$, the first term of $b_n^{(1)}$ admits

$$\left| \sum_{m=-\infty}^{\infty} \left(\int_0^\Lambda e^{i(\beta_n f_{\ell,N} + \alpha_{m-n}x)} \left(e^{i\beta_n(f - f_{\ell,N})} - 1 - i\beta_n (f - f_{\ell,N}) \right) dx \right) B_m \right|$$

$$\lesssim \sum_{m=-\infty}^{\infty} \left| \left(e^{i\beta_n f_{\ell,N}} \left(\widehat{e^{i\beta_n(f-f_{\ell,N})} - 1 - i\beta_n(f - f_{\ell,N})} \right) \right)(m - n) \right| \cdot |B_m|$$

$$\lesssim \left\| e^{i\beta_n f_{\ell,N}} \left(e^{i\beta_n(f-f_{\ell,N})} - 1 - i\beta_n(f - f_{\ell,N}) \right) \right\|_{H^2(0,\Lambda)} \left(|B_n| + \sum_{m=-\infty,m\neq n}^{\infty} \frac{|B_m|}{(m - n)^2} \right)$$

$$\lesssim \left\| e^{i\beta_n f_{\ell,N}} \right\|_{H^2(0,\Lambda)} \left\| e^{i\beta_n(f-f_{\ell,N})} - 1 - i\beta_n(f - f_{\ell,N}) \right\|_{H^2(0,\Lambda)} \left(|B_n| + \sum_{m=-\infty,m\neq n}^{\infty} \frac{|B_m|}{(m - n)^2} \right)$$

$$\lesssim (\tau|\beta_n|)^2 \left(\frac{1}{n^2} + \frac{\epsilon}{|n|^{1/2}} + \sum_{m=-\infty,m\neq 0,n}^{\infty} \frac{\epsilon}{|m|^{1/2}(m - n)^2} \right) \lesssim \tau^2.$$

The second term of $b_n^{(1)}$ satisfies

$$\left| \sum_{|m|>N} \left(\int_0^\Lambda e^{i(\beta_n f_{\ell,N} + \alpha_{m-n} x)} \left(1 + i\beta_n \left(f - f_{\ell,N} \right) \right) dx \right) B_m \right|$$

$$\lesssim \sum_{|m|>N} \left| \left(\widehat{e^{i\beta_n f_{\ell,N}} \left(1 + i\beta_n \left(f - f_{\ell,N} \right) \right)} \right)(m-n) \right| \cdot |B_m|$$

$$\lesssim \left\| \left(e^{i\beta_n f_{\ell,N}} \left(1 + i\beta_n \left(f - f_{\ell,N} \right) \right) \right)'' \right\|_{L^2(0,\Lambda)} \sum_{|m|>N} \frac{|B_m|}{(m-n)^2}$$

$$\lesssim \sum_{|m|>N} \frac{\epsilon^2 |\beta_n|}{|m|^{1/2}(m-n)^2} \lesssim \epsilon^2 |n|^{1/2}.$$

The third term of $b_n^{(1)}$ has

$$\left| i\beta_n \sum_{m=-N}^{N} \left(\int_0^\Lambda e^{i(\beta_n f_{\ell,N} + \alpha_{m-n} x)} \left(f - f_{\ell,N} \right) dx \right) \left(B_m^{(0)} - B_m \right) \right|$$

$$\lesssim |\beta_n| \sum_{m=-N}^{N} \left| \left(\widehat{e^{i\beta_n f_{\ell,N}} \left(f - f_{\ell,N} \right)} \right)(m-n) \right| \cdot |B_m^{(0)} - B_m|$$

$$\lesssim |\beta_n| \cdot \left\| e^{i\beta_n f_{\ell,N}} \left(f - f_{\ell,N} \right) \right\|_{H^2(0,\Lambda)} \left(|B_n^{(0)} - B_n| + \sum_{m=-N, m \neq n}^{N} \frac{|B_m^{(0)} - B_m|}{(m-n)^2} \right)$$

$$\lesssim \tau |\beta_n| \left(\frac{\epsilon^2 N^{1/2} + \tau}{n^2} + \frac{\tau}{|n|^{1/2}} + \epsilon^2 N^{1/2} + \sum_{m=-N, m \neq 0, n}^{N} \frac{\left(\frac{\tau}{|m|^{1/2}} + \epsilon^2 N^{1/2} \right)}{(m-n)^2} \right)$$

$$\lesssim \tau^2 |n|^{1/2} + \frac{\epsilon \tau}{N^{1/2}}.$$

The fourth term of $b_n^{(1)}$ admits

$$\left| i\beta_n \sum_{m=-N}^{N} \int_0^\Lambda B_m^{(0)} \left(f - f_N \right) e^{i(\beta_n f_{\ell,N} + \alpha_{m-n} x)} dx \right|$$

$$\lesssim |\beta_n| \sum_{|k|>N} |C_k| \cdot \left| \int_0^\Lambda e^{i(\beta_n f_{\ell,N} + \alpha_{k-n} x)} dx \right| + |\beta_n| \sum_{m=-N, m \neq 0}^{N} |B_m^{(0)}| \cdot \left| \int_0^\Lambda \left(f - f_N \right) e^{i(\beta_n f_{\ell,N} + \alpha_{m-n} x)} dx \right|$$

$$\lesssim |\beta_n| \sum_{|k|>N} \frac{\epsilon^2 |\beta_n|}{k^2 (k-n)^2} + |\beta_n| \sum_{m=-N, m \neq 0}^{N} \left| \left(\widehat{e^{i\beta_n f_{\ell,N}} \left(f - f_N \right)} \right)(m-n) \right| \cdot |B_m^{(0)}|$$

$$\lesssim \epsilon^2 + |\beta_n| \cdot \left\| e^{i\beta_n f_{\ell,N}} (f - f_N) \right\|_{H^2(0,\Lambda)} \left(B_n^{(0)} + \sum_{m=-N, m \neq 0, m \neq n}^{N} \frac{|B_m^{(0)}|}{(m-n)^2} \right)$$

$$\lesssim \epsilon^2 + |\beta_n| \cdot \| f - f_N \|_{H^2(0,\Lambda)} \left(\frac{\epsilon}{|n|^{1/2}} + \sum_{m=-N, m \neq 0, m \neq n}^{N} \frac{\epsilon}{|m|^{1/2}(m-n)^2} \right)$$

$$\lesssim \epsilon^2 + \epsilon |n|^{1/2} \| f - f_N \|_{H^2(0,\Lambda)}.$$

Similarly, for the case $n = 0$, we have the following estimates for the four terms:

$$\left| \sum_{m=-\infty}^{\infty} \left(\int_0^\Lambda e^{i(\kappa f_{\ell,N} + \alpha_m x)} \left(e^{i\kappa(f - f_{\ell,N})} - 1 - i\kappa \left(f - f_{\ell,N} \right) \right) dx \right) B_m \right|$$

$$\leqslant \tau^2 \left(1 + \sum_{m=-\infty, m\neq 0}^{\infty} \frac{\epsilon^2}{|m|^{5/2}} \right) \lesssim \tau^2,$$

$$\left| \sum_{|m|>N} \left(\int_0^\Lambda e^{i(\kappa f_{\ell,N} + \alpha_m x)} \left(1 + i\kappa \left(f - f_{\ell,N} \right) \right) dx \right) B_m \right|$$

$$\leqslant \sum_{|m|>N} \frac{\epsilon^2}{|m|^{5/2}} \lesssim \epsilon^2,$$

$$\left| i\kappa \sum_{m=-N}^{N} \left(\int_0^\Lambda e^{i(\kappa f_{\ell,N} + \alpha_m x)} \left(f - f_{\ell,N} \right) dx \right) \left(B_m^{(0)} - B_m \right) \right|$$

$$\leqslant \tau \left(\tau + \epsilon^2 N^{1/2} + \sum_{m=-N, m\neq 0}^{N} \frac{\left(\frac{\tau}{|m|^{1/2}} + \epsilon^2 N^{1/2} \right)}{|m|^2} \right) \lesssim \tau^2 + \frac{\epsilon\tau}{N},$$

$$\left| i \sum_{m=-N}^{N} \int_0^\Lambda B_m^{(0)} \left(f - f_N \right) e^{i(f_{\ell,N} + \alpha_{m-n} x)} dx \right|$$

$$\lesssim \epsilon^2 + \|f - f_N\|_{H^2(0,\Lambda)} \sum_{m=-N, m\neq 0}^{N} \frac{\epsilon}{|m|^{5/2}} \lesssim \epsilon \|f - f_N\|_{H^2(0,\Lambda)} + \epsilon^2,$$

which completes the proof.　　　　　　　　　　　　　　　　　　　　　　□

References

[1]　Ammari H 1995 Uniqueness theorems for an inverse problem in a doubly periodic structure *Inverse Problems* **11** 823–33

[2]　Arens T and Kirsch A 2003 The factorization method in inverse scattering from periodic structures *Inverse Problems* **19** 1195–211

[3]　Bao G 1994 A unique theorem for an inverse problem in periodic diffractive optics *Inverse Problems* **10** 335–40

[4]　Bao G 1995 Finite element approximation of time harmonic waves in periodic structures *SIAM J. Numer. Anal.* **32** 1155–69

[5]　Bao G, Cowsar L and Masters W 2001 *Mathematical Modeling in Optical Science* (*Frontiers in Applied Mathematics* vol 22) (Philadelphia: SIAM)

[6]　Bao G, Cui T and Li P 2014 Inverse diffraction grating of Maxwell's equations in biperiodic structures *Opt. Express* **22** 4799–816

[7]　Bao G, Dobson D and Cox J A 1995 Mathematical studies in rigorous grating theory *J. Opt. Soc. Am.* A **12** 1029–42

[8]　Bao G and Friedman A 1995 Inverse problems for scattering by periodic structure *Arch. Ration. Mech. Anal.* **132** 49–72

[9]　Bao G and Li P 2013 Near-field imaging of infinite rough surfaces *SIAM J. Appl. Math.* **73** 2162–87

[10]　Bao G and Li P 2014 Near-field imaging of infinite rough surfaces in dielectric media *SIAM J. Imaging Sci.* **7** 867–99

[11]　Bao G and Li P 2014 Convergence analysis in near-field imaging *Inverse Problems* **30** 085008

[12] Bao G, Li P and Lv J 2013 Numerical solution of an inverse diffraction grating problem from phaseless data *J. Opt. Soc. Am.* A **30** 293–9

[13] Bao G, Li P and Wang Y 2016 Near-field imaging with far-field data *Appl. Math. Lett.* **60** 36–42

[14] Bao G, Li P and Wu H 2012 A computational inverse diffraction grating problem *J. Opt. Soc. Am.* A **29** 394–9

[15] Bao G, Zhang H and Zou J 2011 Unique determination of periodic polyhedral structures by scattered electromagnetic fields *Trans. Am. Math. Soc.* **363** 4527–51

[16] Bao G and Zhou Z 1998 An inverse problem for scattering by a doubly periodic structure *Trans. Am. Math. Soc.* **350** 4089–103

[17] Bruckner G, Cheng J and Yamamoto M 2002 An inverse problem in diffractive optics: conditional stability *Inverse Problems* **18** 415–33

[18] Bruckner G and Elschner J 2003 A two-step algorithm for the reconstruction of perfectly reflecting periodic profiles *Inverse Problems* **19** 315–29

[19] Carney S and Schotland J 2003 Near-field tomography *MSRI Ser. Math. Appl.* **47** 133–68

[20] Chen Z and Huang G 2017 Phaseless imaging by reverse time migration: acoustic waves *Numer. Math. Theor. Meth. Appl.* **10** 1–21

[21] Cheng T, Li P and Wang Y 2013 Near-field imaging of perfectly conducting grating surfaces *J. Opt. Soc. Am.* A **30** 2473–81

[22] Desanto J A 1981 Scattering from a perfectly reflecting arbitrary periodic surface: an exact theory *Radio Sci.* **16** 1315–26

[23] Elschner J, Hsiao G and Rathsfeld A 2003 Grating profile reconstruction based on finite elements and optimization techniques *SIAM J. Appl. Math.* **64** 525–45

[24] Gaylord T K and Moharam M G 1985 Analysis and applications of optical diffration by gratings *Proc. IEEE* **73** 894–937

[25] Gilbarg D and Trudinger N 1983 *Elliptic Partial Differential Equations of Second Order* (New York: Springer)

[26] Grafakos L 2004 *Classical and Modern Fourier Analysis* (Englewood Cliffs, NJ: Prentice Hall)

[27] Hettlich F 2002 Iterative regularization schemes in inverse scattering by periodic structures *Inverse Problems* **18** 701–14

[28] Hettlich F and Kirsch A 1997 Schiffer's theorem in inverse scattering theory for periodic structures *Inverse Problems* **13** 351–61

[29] Hu G, Yang J and Zhang B 2011 An inverse electromagnetic scattering problem for a bi-periodic inhomogeneous layer on a perfectly conducting plate *Appl. Anal.* **90** 317–33

[30] Ito K and Reitich F 1999 A high-order perturbation approach to profile reconstruction: I. Perfectly conducting gratings *Inverse Problems* **15** 1067–85

[31] Jiang X and Li P Inverse electromagnetic diffraction by biperiodic dielectric gratings *Inverse Problems* **33** 085004

[32] Kirsch A 1993 *Diffraction by Periodic Structures* (Berlin: Springer)

[33] Kirsch A 1994 Uniqueness theorems in inverse scattering theory for periodic structures *Inverse Problems* **10** 145–52

[34] Klibanov M V 2017 A phaseless inverse scattering proble for the 3D Helmholtz equation *Inverse Problems Imaging* **11** 263–76

[35] Lechleiter A and Nguyen D L 2013 On uniqueness in electromagnetic scattering from biperiodic structures *ESAIM Math. Modell. Numer. Anal.* **47** 1167–84

[36] Lechleiter A and Nguyen D L 2013 Factorization method for electromagnetic inverse scattering from biperiodic structures *SIAM J. Imaging Sci.* **6** 1111–39

[37] Li J, Liu H and Wang Y 2017 Recovering an electromagnetic obstacles by a few phaseless backscattering measurements *Inverse Problems* **33** 035011

[38] Malcolm A and Nicholls D P 2011 A boundary perturbation method for recovering interface shape in layered media *Inverse Problems* **27** 095009

[39] Nédélec J-C and Starling F 1991 Integral equation methods in a quasi-periodic diffraction problem for the time-harmonic Maxwell's equations *SIAM J. Math. Anal.* **22** 1679–701

[40] Petit R (ed) 1980 *Electromagnetic Theory of Gratings* (New York: Springer)

[41] Uretsky J L 1965 The scattering of plane waves from periodic surface *Ann. Phys.* **33** 400–27

[42] Yang J, Zhang B and Zhang R 2016 Near-field imaging of periodic interfaces in multilayered media *Inverse Problems* **32** 035010

[43] Yang J, Zhang B and Zhang R 2013 Reconstruction of penetrable grating profiles *Inverse Problems Imaging* **7** 1393–407

[44] Zhang B and Zhang H 2017 Imaging of locally rough surfaces from intensity-only far-field or near-field data *Inverse Problems* **33** 055001

[45] Zhang B and Zhang H 2017 Recovering scattering obstacles by multi-frequency phaseless far-field data *J. Comput. Phys.* **345** 58–73

[46] Zhang R and Zhang B 2014 Near-field imaging of periodic inhomogeneous media *Inverse Problems* **30** 045004